universität wien

MASTERARBEIT / MASTER'S THESIS

Titel der Masterarbeit / Title of the Master's Thesis

Characterization of distinct functional domains of Pax5 *in vivo*

verfasst von / submitted by

Sarah Grünbacher, BSc

angestrebter akademischer Grad / in partial fulfilment of the requirements for the degree of

Master of Science (MSc)

Wien, 2017 / Vienna 2017

Studienkennzahl lt. Studienblatt / degree programme code as it appears on the student record sheet:	A 066 830
Studienrichtung lt. Studienblatt / degree programme as it appears on the student record sheet:	Masterstudium Molekulare Mikrobiologie, Mikrobielle Ökologie und Immunbiologie
Betreut von / Supervisor:	Ao. Univ.-Prof. Dr. Meinrad Busslinger

Acknowledgments

First of all, I wish to express my sincere gratitude to Ao. Univ.-Prof. Dr. Meinrad Busslinger for giving me the opportunity to work in his research group, for great support and scientific advices. In addition, I want to thank my direct supervisor Louisa Hill, MSc, for being a great role model and always having patience with me. You taught me a lot about science and I am more than happy that I had the opportunity to work with you. I also want to thank Miriam Wöhner, PhD, who supported me with her knowledge and skills in many experiments. I would also like to express my gratitude towards Daniela Kostanova, PhD, Louisa Hill, PhD and the transgenic mouse service for generating the mouse mutants I analyzed in this study. Next, I want to thank the whole Busslinger group for creating a great working atmosphere. Last but not least, I want to thank my friends and family who supported me during my studies.

Sarah Grünbacher

Table of Contents

Abbreviations

AA	amino acid
AID	activation induced deaminase
ALL	acute lymphoblastic leukemia
BAF	barrier-to-autointegration factor
BCR	B cell receptor
Blimp1	B lymphocyte-induced maturation protein 1
BLNK	B cell linker protein
BM	bone marrow
CBP	CREB-binding protein
CLP	common lymphoid progenitor
CMP	common myeloid progenitor
CRISPR/Cas9	clustered regularly interspaced short palindromic repeat /CRISPR-associated protein
CSR	class switch recombination
DN	double negative
DP	double positive
DSB	double strand break
DTT	Dithiothreitol
EBF1	early B-cell factor 1
ELISA	Enzyme-linked Immunosorbent Assay
ELISPOT	Enzyme Linked Immuno Spot Assay
ERK	extracellular signal–regulated kinases
E2A	immunoglobulin enhancer-binding factors E12/E47
FDC	follicular dendritic cell
Flt3	receptor- type tyrosine- protein kinase
FO	follicular B cells
Foxo1	forkhead box protein O1
HD	partial homeodomain
HSC	hematopoietic stem cells
GC	germinal center
Grg4	groucho- related gene product 4
Gro-seq	global run-on sequencing

ID	inhibitory domain
IgH	immunoglobulin heavy chain
IgL	immunoglobulin light chain
IL7Rα	interleukin 7 receptor alpha
IRF4	interferon regulatory factor 4
KLH	keyhole limpet hemocyanin
LMPP	lymphoid-primed multipotent progenitor
LN	lymph node
LPS	lipopolysaccharide
MACS	magnetic activated cell sorting
MAPK	mitogen-activated protein kinase
MLL	mixed lineage leukemia
MZ	marginal zone B cells
NCoR1	nuclear receptor corepressor 1
NF-κB	nuclear factor kappa-light-chain-enhancer
NK cells	natural killer cells
NP-KLH	4-hydroxy-3-nitrophenyl acetyl–KLH
OP	octapeptid
PAM	protospacer adjacent motif
PAMP	pathogen-associated molecular pattern
Pax5	paired box protein 5
PD	paired domain
PIC	protease inhibitor cocktail
pre-BCR	pre-B cell receptor
PRR	pathogen recognition receptor
RB	retinoblastoma
RSS	recombination signal sequences
sgRNA	single guide RNA
TAD	transactivation domain
Tbp	TATA-binding protein
TCRβ	T cell receptor beta
TLR	toll-like receptor
WT	wild type

Xbp 1	X-box binding protein 1
6AA	6-aminocaproic acid

List of figures

1. Introduction

1.1. The innate vs. the adaptive immune system

Our immune system is constantly challenged by environmental hazards. In order to react to foreign pathogens, the immune system needs to adapt continuously. To do so, this multilayered system is divided into two subsystems, the innate and the adaptive immune system.

A rapid response upon infection is provided by the innate immune system which serves as a non-specific first-line defense mechanism. Cells of the innate immune system are defined by their unique ability to identify self from non-self. These cells are able to recognize pathogen-associated molecular patterns (PAMPS) of pathogens via their pathogen recognition receptors (PRR). PAMPs are unmethylated DNA or structures on the cell walls of bacteria such as lipopolysaccharide (LPS) on gram negative bacteria. The PRR toll-like receptor 4 (TLR4) recognizes LPS and induces an immune response. In addition to cells of the innate immune system, TLR4 is also expressed on B cells which can induce the activation of B cells (Murphy et al. 2007).

The adaptive immune system, on the other hand, is responsible for activation of pathogen-specific lymphocytes. By randomly rearranging their antigen receptors, lymphocytes are able to recognize a hypothetical infinite number of different pathogens. In addition, long-term memory is build up by the adaptive immune system in order to react to pathogens faster upon reinfection. The main players of the adaptive immune response are T and B lymphocytes which provide us with cell-mediated immunity and humoral immunity, respectively. (Busslinger & Tarakhovsky 2014).

1.2. The hematopoietic system

B and T cells are part of the hematopoietic system. The pluripotent hematopoietic stem cells (HSC) in the bone marrow give rise to B and T lymphocytes, natural killer (NK) cells, erythroid and myeloid cells via several developmental steps (Busslinger & Tarakhovsky 2014). HSC can either differentiate into common myeloid progenitors (CMPs) or lymphoid-primed multipotent progenitors (LMPPs). Whereas CMPs are able to differentiate further into the erythroid or myeloid lineage, LMPPs are restricted to develop either into common lymphoid progenitors

(CLPs) or the myeloid lineage. CLPs can subsequently differentiate into NK cells, T cells or B cells (Busslinger & Tarakhovsky 2014; Figure 1).

The early developmental progression of lymphopoiesis needs to be under tight control in order to assure accurate lineage commitment. Each developmental step exhibits a unique gene expression signature. Hence, a multitude of signals are involved in the generation of CLPs (Busslinger & Tarakhovsky 2014). The receptor- type tyrosine- protein kinase (Flt3) is expressed on LMPPs and is essential for the differentiation into CLPs (Adolfsson et al. 2005). Next to Flt3, signaling through c-Kit, IL-7 receptor, Ikaros and PU.1 are crucial for CLP development (Nutt & Kee 2007).

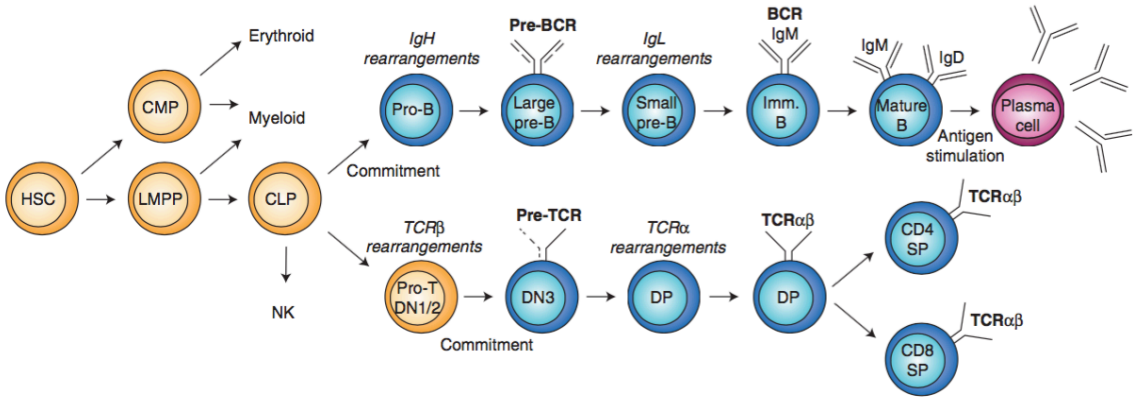

Figure 1. Schematic drawing of B and T lymphopoiesis.
Hematopoietic stem cells (HSC) give rise to common myeloid progenitors (CMPs) and lymphoid-primed multipotent progenitors (LMPPs)**.** LMPPs are able to differentiate into common lymphoid progenitors (CLP)s which subsequently undergo either B or T cell lineage commitment or differentiate into natural killer cells (NK cells). Pro-B cells develop along the B cell pathway until the high- affinity antibody producing plasma cells stage. (Busslinger & Tarakhovsky 2014)

1.3. Early B cell development

Multiple transcription factors such as immunoglobulin enhancer-binding factors E12/E47 (E2A) (Zhuang et al. 1994), early B-cell factor 1 (EBF1) (Lin & Grossschedl, 1995) and the paired box protein 5 (Pax5) (Nutt et al. 1999) have been shown to play a role in the highly complex process of B cell lineage entry and maintenance of B lymphocyte identity.

The earliest stage of B cell precursors was previously described as the pre-pro-B cell which is characterized by the expression of the B cell surface marker B220 (Li et al. 1996). In addition, surface markers such as Flt3, IL7Rα, Ly6D and c-Kit have been shown to be expressed by pre-pro-B cells (Inlay et al. 2009). However, the B cell specific transcription factor Pax5 is barely

detectable in pre-pro-B cells which suggests that they are not fully committed to the B cell lineage and are still able to differentiate into other hematopoietic lineages (Nagasawa 2006).

The transition from pre-pro-B cells to pro-B cells is controlled by EBF1, E2A and forkhead box protein O1 (Foxo1). They regulate the expression of B lymphocyte specific genes (Y. C. Lin et al. 2010). In addition, Pax5 tailors the gene expression profile of early B cell precursors by activating B cell-specific genes and simultaneously repressing B cell-unspecific genes throughout B lymphopoiesis (Nutt et al. 1999). Target genes which are activated by Pax5 are *Cd79a*, *Cd19* and *B cell linker protein* (*Blnk*) (Cobaleda et al. 2007). The expression of these genes contributes to further B cell developments since they are involved in pre-B cell receptor (pre-BCR) and BCR signaling. Furthermore, Pax5 induces the expression of genes involved in cell adhesion, migration and V_H-DJ_H recombination at the immunoglobulin heavy chain (IgH) locus (Cobaleda et al. 2007). On the other hand, Pax5 represses signals which would lead to development to other lymphoid, erythroid or myeloid lineages such as *Notch1* or *colony stimulating factor 1 receptor* (*Csf1r*) (Delogu et al. 2006). Hence, the development from pro- B cells to mature B cell is under the tight control of by Pax5 (Figure 1).

In pro-B cells, gene segments coding for the heavy chain of the B cell receptor (BCR) are rearranged, and together with a surrogate light chain, form the pre-BCR. This leads to the transition to the next developmental stage, the pre-B cell (see 1.3.1). Subsequently, rearrangement of the immunoglobulin light chain (IgL) in pre-B cells induces the development to immature B cells (see 1.3.1). Immature B cells are defined by their expression of IgM which is the first expressed isotype of the BCR. As a next step, immature B cells migrate into secondary lymphoid organs (spleen, lymph nodes) where they undergo their next transition to mature B cells. Only upon encounter with an antigen, mature B cells get activated and differentiate into high affinity antibody producing plasma cells (Murphy et al. 2007; see 1.3.2).

1.3.1. V(D)J recombination

The key function of B lymphocytes is to recognize pathogens in order to induce their destruction via a highly complex signaling network which involves a multitude of different cell types. The recognition of the pathogen is ensured via the BCR. The BCR is a transmembrane protein which is composed of the immunoglobulin heavy chain (IgH) and the immunoglobulin light chain Igκ/Igλ (IgL). The IgH is encoded by variable (V), diversity (D) and joining (J) gene segments, whereas the IgL is encoded by V and J gene segments only. These segments are rearranged in a highly ordered process by a mechanism termed V(D)J recombination in the

course of B cell development. This leads to the generation of a highly diverse immune repertoire (Murphy et al. 2005).

A key player in V(D)J recombination is the RAG recombinase which is part of the V(D)J recombinase protein complex. RAG is a heterodimer of Rag1 and Rag2 and recognizes recombination signal sequences (RSS), which are distinct sequences flanking the gene segments. RAG generates double strand breaks (DSBs), the ends of which are subsequently processed and joined by non-homologous end-joining (Murphy et al. 2007).

The *IgH* locus is rearranged in pro-B cells, followed by rearrangement of *Igκ/Igλ* in pre-B cells. First, DJ_H rearrangements are induced between gene segments which are in close proximity to each other. Subsequently, the *IgH* locus undergoes contraction in order to ensure V-DJ recombination of distal V genes (Murphy et al. 2007).

However, point mutations and frameshift mutations can occur during V(D)J recombination, leading to unsuccessful rearrangements. Hence, B lymphocytes must pass several checkpoints in order to eliminate non-functional or self-reactive BCRs. Therefore, the heavy chain protein forms in combination with a surrogate light chain, the pre-BCR in pro-B cells. Only cells expressing a functional pre-BCR are able to proliferate and transit to pre-B cell in which the light chain locus is rearranged (Murphy et al. 2007).

At the *Igκ/Igλ* loci rearrangement occurs between V and J gene segments, since the light chain loci do not contain D segments. If the rearrangement was successful, the pre-B cells develop into immature B cell which is able to express IgM on its surface. If the recombination of the gene segments did not result in a functional light chain protein or resulted in recognition of self-antigens, the cells are eliminated by apoptosis. Functional immature B cells subsequently migrate to secondary lymphoid organs where they can get activated and are able to undergo a second round of editing (Murphy et al. 2007; see 1.4).

1.4. Late B cell development

B lymphocytes originate in the bone marrow. In later B cell development, they migrate into secondary lymphoid organs such as spleen or lymph nodes. Upon activation of B cells, proliferation and differentiation is induced (Figure 1). In addition, mature B cells undergo a second round of mutation of their antigen receptors in order to develop further into high-affinity antibody secreting plasma cells and memory B cells (De Silva & Klein 2015).

Germinal centers (GCs) are transient structures formed in the follicle of secondary lymphoid organs. These structures during a germinal center reaction contain follicular dendritic

cells (FDC) and B cells. In addition, the follicle is surrounded by T cells which form the T cell zone. The GC is organized in a dark zone (DZ) and a light zone (LZ). The DZ is densely populated by B cells which is not the case for the LZ, where also other cell types are located such as FDC and T_{FH} cells (De Silva & Klein 2015).

1.4.1. Activation of B cells

To initiate a GC reaction, a multitude of different cell types are involved in signaling through a complex cascade to activated naïve B cells. Follicular B cells retrieve antigen presented from FDCs (Shikh et al. 2010). Subsequently, the antigen is internalized and processed. At the border between T cell zone and B cell zone, follicular B cells present the processed antigen to $CD4^+$ T follicular helper cells (T_{FH}) via peptide- MHCII interaction. This induces the activation of the T cells which subsequently express CD40L on their surface. The follicular B cells express CD40 which in turn binds to its ligand on T cells. These long-lived interaction leads to proliferation and differentiation of the B cells in order to boost the immune reaction (Parker et al. 1993; De Silva & Klein 2015). In addition, B cells can also get activated without T cell help by binding of an antigen directly to the BCR receptor (Murphy et al. 2007).

1.4.2. The Germinal center reaction

As it has been described earlier (see 1.3.1.), the generation of antigen receptors in B cells occurs via V(D)J recombination in the early stages of B cell development. However, a second round of modifications is essential to generate more diverse antibodies. After activation of B cells, they migrate into the DZ of the GC and undergo several rounds of cell division (clonal expansion) followed by somatic hypermutation (SHM) and class switch recombination (CSR) in the LZ to modify the immunoglobulin receptors of the activated B cells. SHM induces a high rate of mutations in the variable regions of the BCR in order to produce a highly diverse repertoire of antibodies. (Murphy et al. 2007). The main player of SHM and CSR is the protein activation induced deaminase (AID) which is induced upon BCR signaling. AID mediates cytosine to uracil mutations in the immunoglobulin loci (Maul & Gearhart 2010). Self-reactive or non-reactive mature B cells undergo apoptosis. Only B cells with high affinity antigen-binding potential are selected in the LZ and differentiate into plasma cells or memory B cells as a final stage of the germinal center reaction (De Silva & Klein 2015).

Whereas SHM leads to the generation of highly diverse antibodies, CSR generates various isotypes of immunoglobulin such as IgG, IgE or IgA which exhibit different types of effector functions. The switching to the different Ig isotypes depends on cytokine signaling and mediates the reaction of the B lymphocytes to different types of environmental hazards. CSR takes place in the LZ of the GC and changes only the constant regions of the IgH, whereas the variable regions stay unaltered. The recombination of the constant segments is not random and depends on signals from helper T cells and other cells. This enables an activated B cell to give rise to different daughter cells producing varying antibodies with different isotypes (Murphy et al. 2007).

1.4.3. Plasma cells and memory B cells

Plasma cells can be generated by B1 cells, marginal zone B cells or follicular B cells. In contrast to plasma cells derived from follicular B cells, activated B1 and marginal zone B cells do not dependent on T cell help for plasma cell generation. However, they can only give rise to short-lived plasma cells which secrete low-affinity antibodies (Nutt et al. 2015).

Follicular B cells, on the other hand, can either differentiate into short-lived plasma cells by exiting the GC rapidly or they can transition into long-lived plasma cells. These cells are defined by their secretion of high-affinity antibodies in order to eliminate a specific evading foreign pathogen. The transition of terminally differentiated B cells into plasma cells is under the control of B lymphocyte-induced maturation protein 1 (Blimp1) (Murphy et al. 2007). Blimp1 is a transcriptional repressor which regulates the plasma cell differentiation by repressing *c-Myc* (Lin et al. 1997), *Pax5* (Lin et al. 2002) and *CIITA* (Piskurich et al. 2000). Recently, it has been shown that Blimp1 also functions as a transcriptional activator (Minnich et al. 2016). C-myc is involved in cell proliferation and growth, and the repression of *CIITA* results in downregulation in MHC class II genes. As stated previously, Pax5 is important for B cell development and maintenance of B cell identity (Horcher et al. 2001; Cobaleda et al. 2007). Pax5 and Blimp1 expression is mutually exclusive, whereas Pax5 controls the expression profile of B cells, Blimp1 regulates the expression of genes essential for plasma cell differentiation (Lin et al. 2002). Yasuda et al. proposes that extracellular signal–regulated kinases 1/2 (ERK1/2)-dependent phosphorylation of Pax5 leads to derepression of Blimp1 which in turn induces repression of Pax5 (Yasuda et al. 2012; see 1.9.1).

As a terminal step of B cell activation, B lymphocytes can also differentiate into memory B cells in a GC-dependent and independent manner. These memory cells divide at a

very low rate and are defined by their unique ability to get rapidly reactivated upon exposure to an antigen they have encountered before. This results in a prompt elimination of pathogens upon reinfection and serves as an immunological memory (Kurosaki et al. 2015).

1.5. Pax5 and its role in early B cell development

As stated previously, B cell lineage entry, commitment and maintenance are controlled by multiple transcription factors such as E2A (Zhuang et al. 1994), EBF1(Lin & Grossschedl, 1995) and Pax5 (Nutt et al. 1999; Horcher et al. 2001; Cobaleda et al. 2007).

Previously, numerous studies found evidence that Pax5 is a key component in orchestrating B cell lineage commitment (Nutt et al. 1999). In the hematopoietic system, the exclusive expression of the transcription factor is initiated in B cells at the pre-pro-B cells stage and declines in activated B cells (Fuxa et al. 2007). It has been shown that Pax5 is important for V-DJ rearrangements and is involved in locus contraction of the IgH locus (Fuxa et al. 2004). Moreover, Pax5 is a conserved transcription factor which is also essential for midbrain development and is expressed in adult testis in mice (Adams et al. 1992).

Nutt et al., showed that Pax5-deficient mice are blocked at an early pro-B cell stage (Nutt et al. 1997). Pax5-deficient cells are c-Kit$^+$ B220$^+$ but do not express CD19 on their surface. Moreover, Pax5-deficient cells are not committed to the B cell lineage since they can differentiate into T lymphocytes, macrophages, granulocytes, dendritic cells, osteoclasts and NK cells *in vitro* in the presence of lineage-specific cytokines in the medium (Nutt et al. 1999) (Cobaleda et al. 2007; Figure 2). In addition, if Pax5-deficient pro-B cells are transplanted into mice they are able to give rise to cells of other hematopoietic lineages *in vivo* (Rolink et al. 1999; Schaniel et al. 2002) (Figure 2). Pax5 deficiency also leads to a severe growth retardation in mice which die at weaning age (Urbánek et al. 1994) .

Pax5 not only controls B cell lineage commitment but also ensures maintenance of B cell identity by functioning in a dual way. Pax5 controls the gene expression of the early B cell precursors by activating B cell-specific genes and simultaneously repressing B cell-unspecific genes (Nutt et al. 1999; see 1. 3.). Hence, Pax5 on one hand establishes a network of proteins essential throughout the B cell development but on the other hand ensures the inhibition of the expression of B cell inappropriate genes (Medvedovic et al. 2011).

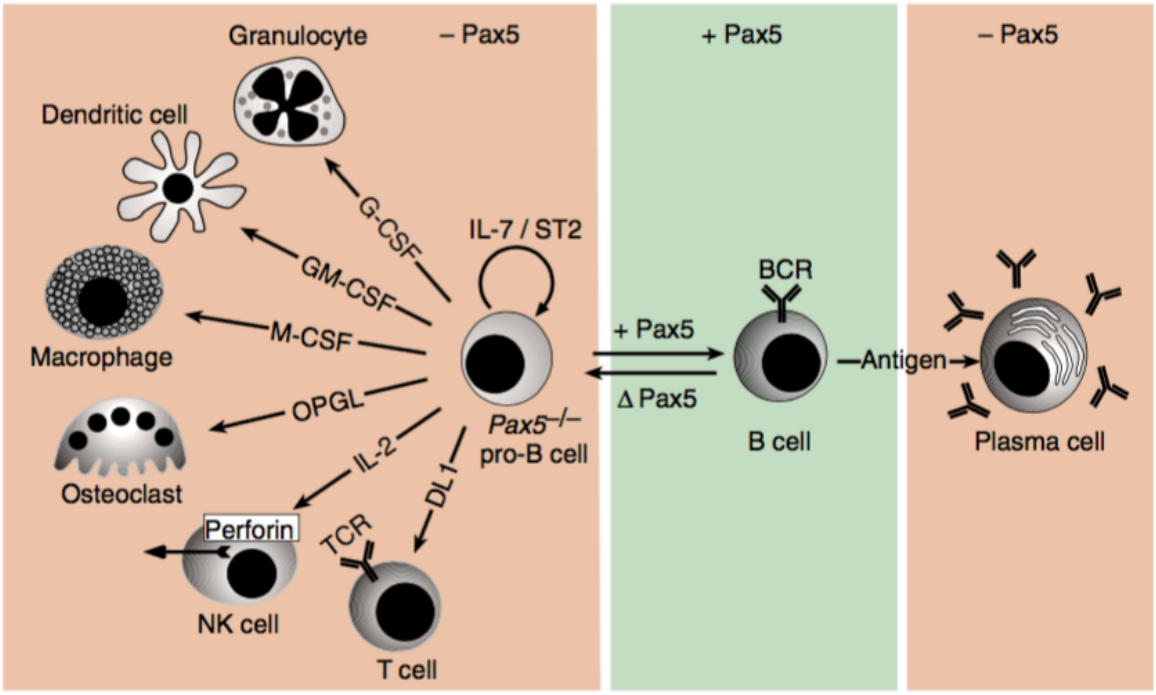

Figure 2. Pax5 is essential for B cell lineage commitment.
Pax5 maintains the B cell lineage commitment by activating B cell-specific genes and repressing B cell-unspecific genes. Pax5 is expressed during B cell development until the plasma cell stage. Upon deletion of Pax5, B cells are arrested in an early pro-B cell stage and can differentiate into other hematopoietic lineages in the presence of the indicated cytokines (Cobaleda et al. 2007).

1.6. Pax5 and its role in late B cell development

As already described above, Pax5-deficient cells are blocked at an early stage in the B cell lineage. Hence, it was difficult to study the role of Pax5 in later stages of B cell development. Horcher et al. generated a mutant mouse strain containing a *Pax5* floxed conditional allele. With *CD19-Cre* mice, it was possible to study the role of Pax5 in later stages of B lymphopoiesis (Horcher et al. 2001). *CD19-Cre* is expressed from the pro- B cell stage until mature B cells (Rickert et al. 1997). The Cre-mediated deletion of the floxed *Pax5* gene increases upon B cell development parallel to CD19 expression (Schwenk et al. 1997).

In $Pax5^{fl/-}$ *CD19-Cre* mice, Horcher et al. observed the loss of mature B cells and reduced IgG levels in the serum. In addition, B cell specific genes were downregulated, whereas B cell unspecific genes were activated. Hence, they concluded that Pax5 is not only important for B cell lineage commitment but its presence is also essential for maintenance of B cell identity (Horcher et al. 2001).

Furthermore, Cre-mediated deletion of Pax5 was performed in mature B cells *in vitro*, followed by transfer into RAG-2 deficient recipient mice. These Pax5-deficient cells were able to differentiate back to progenitor cells and migrate to the thymus in which they gave rise to T cells *in vivo* (Cobaleda et al. 2007).

Recently, *Pax5*$^{fl/-}$ *CD23 Cre* mice were analyzed in the Busslinger group. A conditional deletion of Pax5 in mature B cells causes a significant reduction of marginal zone (MZ) B cells in the spleen (M. Busslinger, unpublished data).

Taken together, these studies provide evidence that Pax5 is not only important for B cell lineage entry but also throughout B cell development in order to maintain B cell identity.

1.7. The structure of Pax5

Pax5 is composed of 391 amino acids which corresponds to a 42 kDa protein. The transcription factor is organized in five domains: the paired domain (PD), the octapeptide (OP), the partial homeodomain (HD), the transactivation domain (TAD) and the inhibitory domain (ID) (Figure 3A). It is known that the PD is important for DNA binding, the OP and HD ensure protein interaction and the C-terminal TA and ID are essential for gene expression (Dörfler et al. 1996; Eberhard et al. 1999). However, analysis on the contribution of the individual domains has only been performed *in vitro* so far.

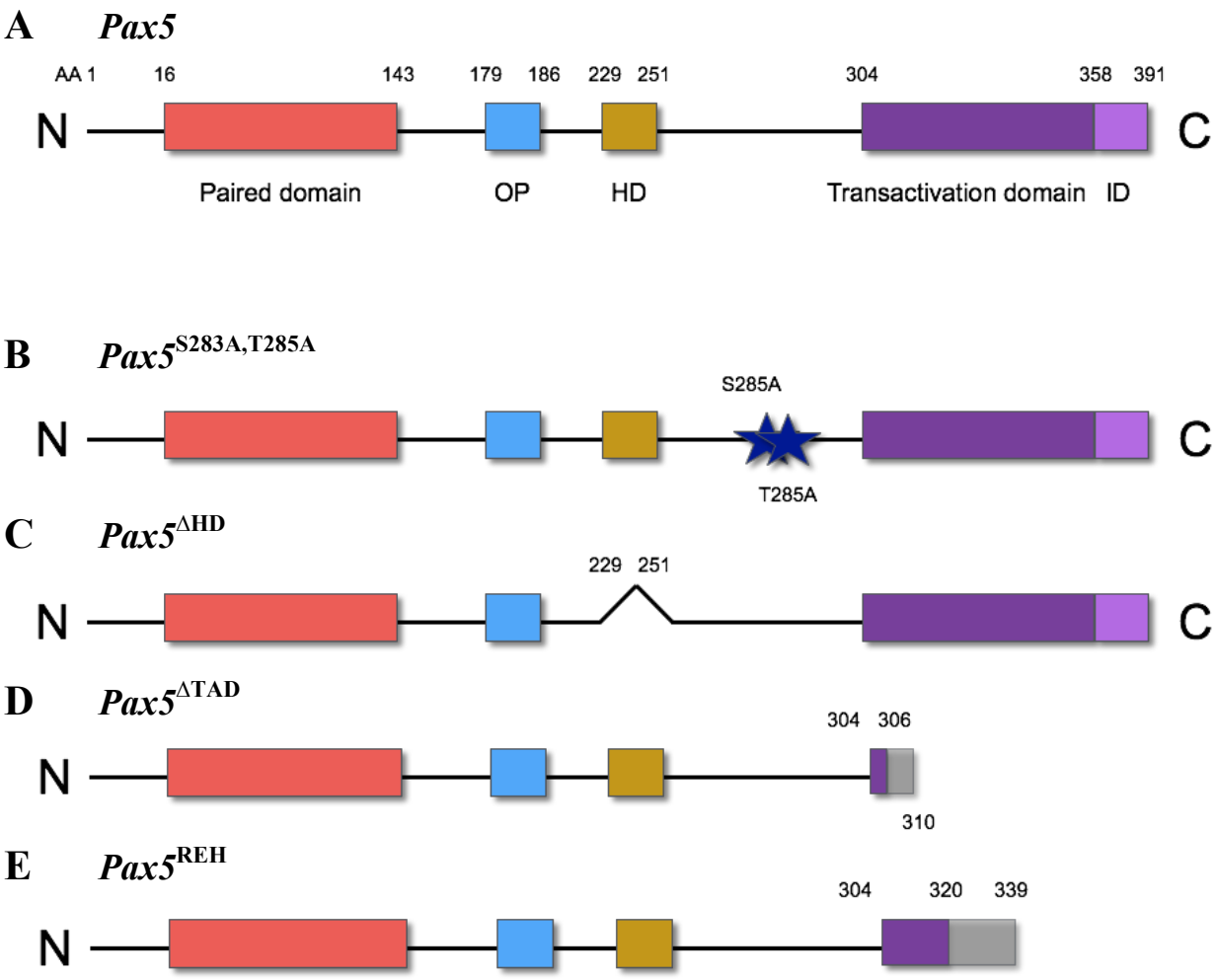

Figure 3. Schematic representation of Pax5 structural organization and the Pax5 mutants analyzed in this study.

(A) Pax5 is composed of 391 amino acids (AA). The transcription factor contains the paired domain, the octapeptide (OP), the partial homeodomain (HD), the transactivation domain and the inhibitory domain (ID). Each number indicates the amino acids of the beginning and end of the Pax5 domains. (B) The *Pax5*^{S283A,T285A} allele is mutated at serine 283 and threonine 285. (C) For the *Pax5*$^{\Delta HD}$ allele, the partial homeodomain (AA 229-AA 251) was deleted in frame (D). A cysteine insertion in the *Pax5*$^{\Delta TAD}$allele leads to a frameshift at AA 306 which results in a truncated Pax5 protein at AA 310. The box in grey represents the frameshift induced by the point mutation. (E) In the *Pax5*^{REH} allele, a frameshift mutation found in an acute lymphoblastic leukemia patient cell line at AA 320 results in a truncated Pax5 protein at the C- terminal transactivation domain at amino acid 339. The box in grey represents the frameshift induced by the point mutation.

1.8. Aim of this study

The aim of my master's thesis project is to characterize and identify the function of individual Pax5 domains *in vivo* using Pax5 mutant mice. To do so, four different mutant mouse strains have been generated. For one, two mitogen-activated protein kinase (MAPK) phosphorylation sites have been mutated, one mutant was generated by in frame deletion of the partial homeodomain and two mutants contain different truncations of the C- terminal TAD (Figure 3B-E).

1.9. Pax5 mutants analyzed in this study

1.9.1. The *Pax5*^{S283A,T285A} mutant

Previously, two MAPK phosphorylation sites were identified in Pax5. Hela cells were infected with the vaccinia virus that contained a tagged Pax5 protein. Subsequently, tryptic peptides were purified. Heavily phosphorylated sites in Pax5 at S283 and T285 were identified by mass spectrometry and sequencing (M. Busslinger, unpublished data). Since no further analysis of these phosphorylation sites has been performed so far, a mutant mouse strain was generated in which serine 283 and threonine 285 were mutated to alanine in order to prevent phosphorylation of Pax5 *in vivo*. Thus, it was possible to examine the impact of these Pax5 phosphorylation sites on B cell development and function (Figure 3B).

Recently, Yasuda et al. stated that Pax5 phosphorylation is induced by ERK1/2 signaling through BCR stimulation. They claimed that Pax5 was phosphorylated at serines 189 and 283 *in vitro* which results in derepression of the Blimp1 gene. Hence, they hypothesized that phosphorylation of Pax5 is essential for inducing the initial steps in plasma cell differentiation (Yasuda et al. 2012). This finding suggested that at least the phosphorylation of serine 283 might play an important role in Pax5-dependent functions.

1.9.2. The *Pax5*$^{\Delta HD}$ mutant

The partial homeodomain is located in the center of the Pax5 protein at amino acids 229-251 (Figure 3A). The HD is highly conserved throughout evolution and in the Pax family since it is present in other Pax family members such as Pax2 and Pax8 (Eberhard et al. 1999). Studies revealed that the HD mediates binding to the TATA-binding protein (TBP) in COS7 cells and retinoblastoma (RB) *in vitro* via GST-pull down assays (Eberhard et al. 1999). With this

finding, Eberhard et al. claimed that Pax5 is able to be in direct contact with the transcription machinery since TBP mediates initiation of transcription. They also hypothesized that Pax5 activity is controlled by RB which plays an essential role in cell proliferation (Eberhard et al. 1999).

Nevertheless, how the HD contributes to the multiple functions of Pax5 *in vivo* still remains elusive. Based on this, a Pax5 mutant was generated in which the HD is deleted in frame to study the role of the HD more closely (Figure 3C).

1.9.3. The *Pax5*$^{\Delta TAD}$ and *Pax5*^{REH} mutants

The transactivation domain of Pax5 is located at amino acids 304-358 (Dörfler et al. 1996; Figure 3A). This was revealed by transient transfection assays in B cell lines *in vitro*, analyzing Pax5-dependent transactivation potential in numerous C-terminal and internal deletion mutants of Pax5. Three copies of the high affinity Pax5 binding site derived from the CD19 promotor were inserted upstream to the TATA binding box of the rabbit ß-globin gene. Subsequently, B cell lines were transiently transfected with the reporter gene together with the mutant Pax5 expression plasmids. The Pax5-dependent transactivation potential was analyzed by RNase protection analysis (Dörfler et al. 1996). If more than 13 amino acids were deleted from the TA, Pax5-dependent transactivation potential was lost. Interestingly, Pax5 mutants with internal Pax5 deletions, displayed normal transactivation (Dörfler et al. 1996).

In addition, Dörfler et al. generated a Pax5 mutant, mimicking the natural occurring frameshift mutation found in the acute lymphoblastic leukemia (ALL) patient cell line REH. The reading frameshift is generated by an additional cytosine in a series of 7 cytosines which leads to a premature stop codon at amino acid 339. *In vitro* experiments revealed that the truncation of Pax5, identified in the REH cell line, was sufficient to reduce the transactivation by Pax5 by a factor of 4 (Dörfler et al. 1996).

Numerous studies have been performed in order to identify how Pax5 functions as an activator or repressor and therefore mediates B cell development and maintenance of B cell identity. As described above, Eberhard et al. showed that TBP, which is involved in the initiation of transcription, binds to the HD of the Pax5 protein (Eberhard et al. 1999; see 1.9.2). Moreover, mass spectrometry analysis revealed that Pax5 interacts with the partner proteins barrier-to-autointegration factor (BAF), mixed lineage leukemia (MLL), CREB-binding protein (CBP) and nuclear receptor corepressor 1 (NCoR1), which are involved in chromatin remodeling, H3K4 methylation, histone acetylation and histone deacetylation, respectively

(McManus et al. 2011). In addition, it has been shown that Pax5 recruits the corepressor groucho-related gene product 4 (Grg4) to a promotor in order to function as a transcriptional repressor. *In vitro* studies identified that Pax5 interacts with Grg4 via its octapeptide and the TAD (Eberhard et al. 2000). In summary, this provided evidence that Pax5 controls its target genes not only at a transcriptional but also at an epigenetic level.

However, the role of the TAD has only been investigated *in vitro* so far and mostly under Pax5-overexpressing conditions. Hence, we wanted to examine the function of the TAD and its impact on B cell lymphopoiesis *in vivo* more closely. Two truncated Pax5 mutant mouse strains were generated. The first one contains a premature stop codon at the beginning of the TAD at amino acid 311 (Figure 3D). The second one mimics the Pax5 mutation identified in the ALL cell line REH described above at amino acid 339 (Figure 3E). Thus, the two Pax5 mutants truncate the C-terminal TAD to different degrees.

2. Results

2.1. Generation of the *Pax5*^{S283A,T285A} allele

Previously, two MAPK phosphorylation sites have been identified at serine 283 and threonine 285 of Pax5, which are located in exon 7 of Pax5 (M. Busslinger, unpublished data; see 1.9.1.). Hence, these two amino acids were mutated to alanine in the *Pax5*^{S283A,T285A} allele in order to prevent Pax5 phosphorylation (Figure 4A). The *Pax5*^{S283A,T285A} allele was generated by clustered regularly interspaced short palindromic repeat/CRISPR-associated protein (CRISPR/Cas9)-mediated engineering in murine zygotes. In order to prevent the CRISPR/Cas9 protein from further genome editing in the already successfully mutated *Pax5* gene, the protospacer adjacent motive (PAM) was destroyed with the repair template encoding the mutant allele. This resulted in the generation of a restriction site which was used for genotyping of PCR amplified DNA of the mice. For the generation of the *Pax5*^{S283A,T285A} allele, the restriction site BglI was introduced which leads, after restriction digest, to a wild type (WT) fragment of 767-bp and two mutant fragments of 259-bp and 508-bp (Figure 4B). In addition to PCR-based genotyping, the two mutations were verified by Sanger Sequencing (Figure 4C).

A ***Pax5***^{S283A,T285A}

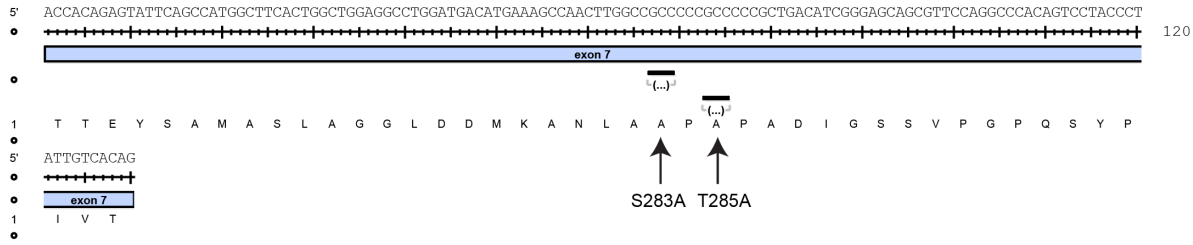

B **Genotyping**

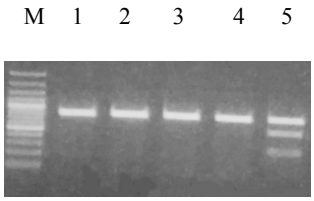

C **Sanger sequencing**

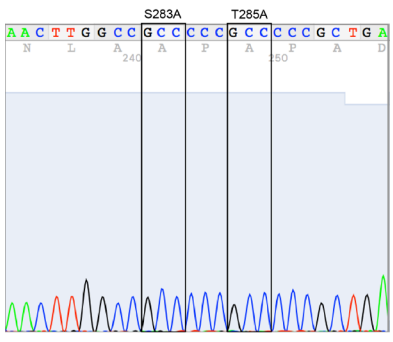

Figure 4. Generation of the *Pax5*^{S283A,T285A} allele.
(A) The sequence of exon 7 of *Pax5* is displayed and the exact position of the mutated amino acids are indicated. (B) Gel electrophoresis picture of genotyping of *Pax5*^{S283A,T25A8} mutant mice. 100-bp ruler was used as a marker (M). *Pax5*$^{+/+}$ fragment (lane 1-4) is 767-bp and *Pax5*$^{S283A,T285A/+}$fragment in lane 5 shows the WT band and two mutant bands of 259-bp and 508-bp. (C) Sanger sequencing of the *Pax5*^{S283A,T285A} mutant PCR fragment. The mutations S283A and T285A are highlighted by the black boxes.

2.1.1 Normal B cell development in *Pax5*$^{S283A,T285A/S283A,T285A}$ mice

To investigate whether the loss of phosphorylation at the two MAPK phosphorylation sites S283 and T285 interferes with the Pax5-dependent B cell development, B lymphocyte populations were examined in the bone marrow (Figure 5A, B) and spleen (Figure 5C, D) via flow cytometry. In addition, T cells in the spleen (Figure 5D) and thymus (Figure 5E) were analyzed.

For flow cytometric analysis, B cells were identified as B220- and CD19- expressing cells. No difference in IgM$^+$ immature B cells (Imm. B), IgD$^+$ mature B cells (Mat. B), IgM$^-$ IgD$^-$ CD2$^+$ pre-B cells and IgM$^-$ IgD$^-$ c-Kit$^+$ pro-B cells could be detected in the bone marrow of *Pax5*$^{S283A,T285A/+}$ and *Pax5*$^{S283A,T285A/S283A,T285A}$mice compared to WT mice (Figure 5A) as well as by calculation of total cell numbers (Figure 5B). In addition, normal B cell development was observed in the spleen of *Pax5*$^{S283A,T285A/+}$ mice and *Pax5*$^{S283A,T285A/S283A,T285A}$ mice (Figure 5C,D). T cell development was not affected by the S283A and T285A mutation (Figure 5E).

To examine the expression levels of Pax5 in the mutant cells, intracellular staining of Pax5 was performed and subsequently analyzed by flow cytometry. *Pax5*$^{\Delta/\Delta}$ B cells were used as a negative control. No difference in the expression profile of Pax5 in *Pax5*$^{S283A,T285A/+}$ B cells and *Pax5*$^{S283A,T285A/S283A,T285A}$ B cells compared to WT could be detected (Figure 5F).

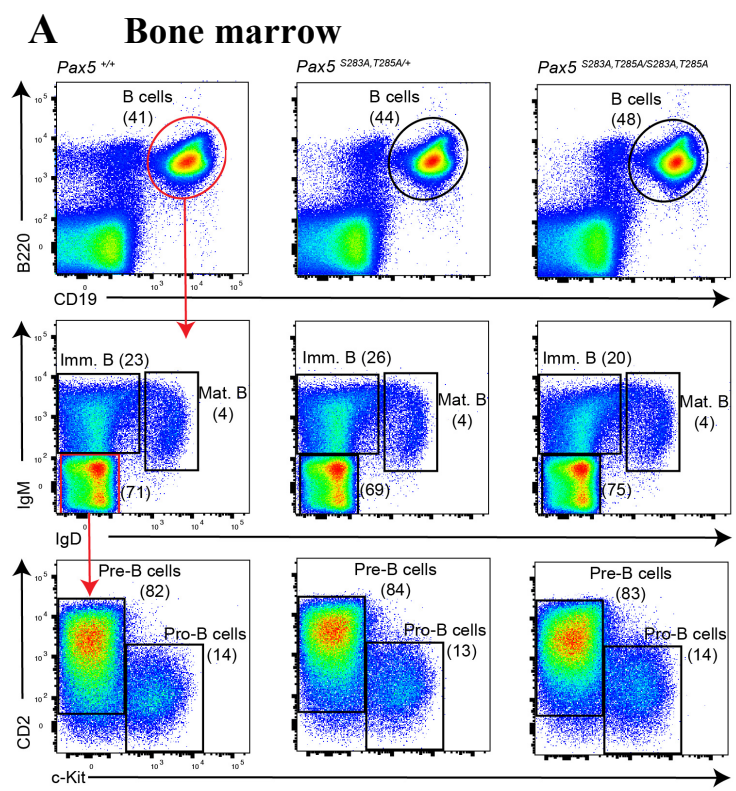
A
Bone marrow
Pax5 +/+
Pax5 S283A,T285A/+
Pax5 S283A,T285A/S283A,T285A
B cells (41)
B cells (44)
B cells (48)
B220
CD19
Imm. B (23)
Mat. B (4)
(71)
Imm. B (26)
Mat. B (4)
(69)
Imm. B (20)
Mat. B (4)
(75)
IgM
IgD
Pre-B cells (82)
Pro-B cells (14)
Pre-B cells (84)
Pro-B cells (13)
Pre-B cells (83)
Pro-B cells (14)
CD2
c-Kit

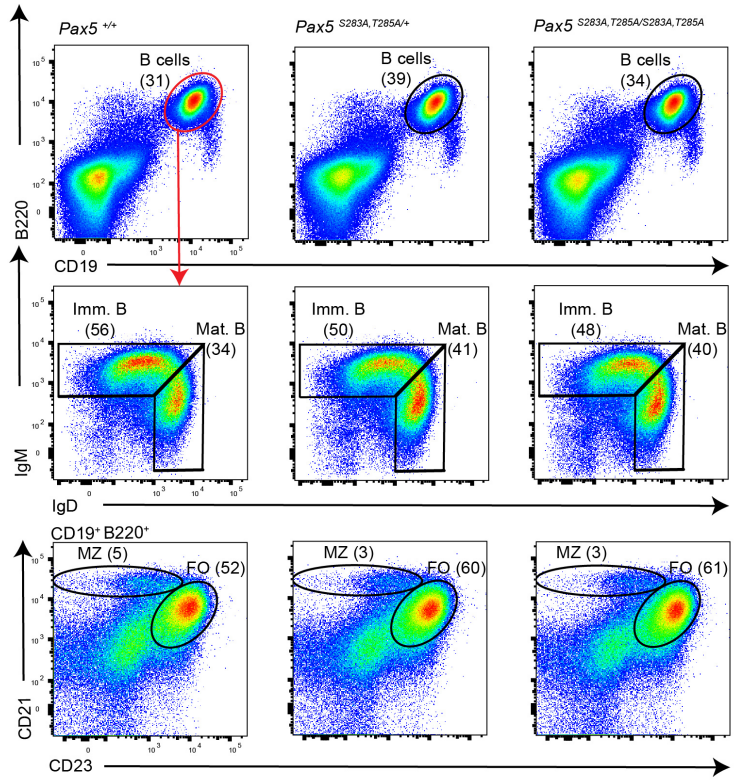
B
Spleen
Pax5 +/+
Pax5 S283A,T285A/+
Pax5 S283A,T285A/S283A,T285A
B cells (31)
B cells (39)
B cells (34)
B220
CD19
Imm. B (56)
Mat. B (34)
Imm. B (50)
Mat. B (41)
Imm. B (48)
Mat. B (40)
IgM
IgD
CD19+ B220+
MZ (5)
FO (52)
MZ (3)
FO (60)
MZ (3)
FO (61)
CD21
CD23

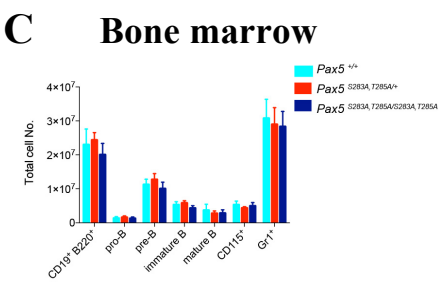
C
Bone marrow
Total cell No.
Pax5 +/+
Pax5 S283A,T285A/+
Pax5 S283A,T285A/S283A,T285A
CD19+ B220+
pro-B
pre-B
immature B
mature B
CD115+
Gr1+

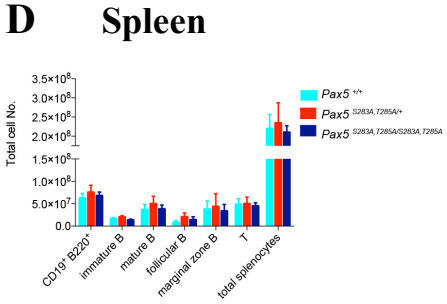
D
Spleen
Total cell No.
Pax5 +/+
Pax5 S283A,T285A/+
Pax5 S283A,T285A/S283A,T285A
CD19+ B220+
immature B
mature B
follicular B
marginal zone B
T
total splenocytes

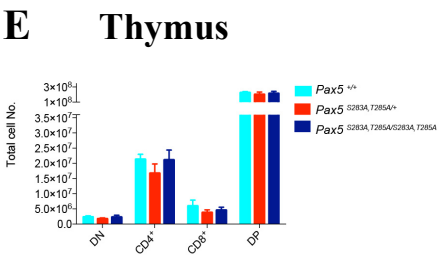
E
Thymus
Total cell No.
Pax5 +/+
Pax5 S283A,T285A/+
Pax5 S283A,T285A/S283A,T285A
DN
CD4+
CD8+
DP

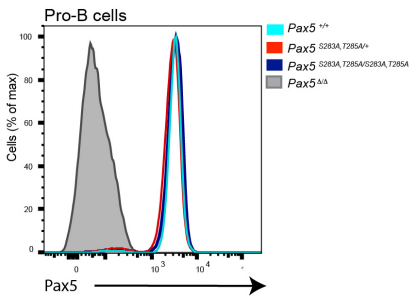
F
Bone marrow
Pro-B cells
Cells (% of max)
Pax5 +/+
Pax5 S283A,T285A/+
Pax5 S283A,T285A/S283A,T285A
Pax5 Δ/Δ
Pax5

Figure 5. Normal B cell development in *Pax5*$^{S283A,T285A/S283A,T285A}$ mice.
Representative flow cytometric analysis of *Pax5*$^{+/+}$, *Pax5*$^{S283A,T285A/+}$ and *Pax5*$^{S283A,T285A/S283A,T285A}$ mice of either bone marrow (BM) (A) or spleen (B). 4-8 week-old littermates were analyzed. Numbers in brackets indicate the percentage of cells in the respective gate. (C-E) Statistical analysis of total cell numbers of different B cell subsets and T cell populations of BM (C), spleen (D) and thymus (E). Error bars indicate mean ± S.E.M., *Pax5*$^{+/+}$ n=4, *Pax5*$^{S283A,T285A/+}$ n=6, *Pax5*$^{S283A,T285A/S283A,T285A}$ n=7. (f) Histogram of Pax5 expression in CD19^{+}B220^{+}IgM^{-}IgD^{-}c-Kit^{+} pro-B cells of the indicated genotype.

2.1.2 Decreased levels of IgG3 and delayed cell proliferation upon LPS stimulation of *Pax5*$^{S283A,T285A/S283A,T285A}$ B cells

Since no phenotype could be detected in unchallenged *Pax5*$^{S283A,T285A/\ S283A,T285A}$ mice, mature B cells were stimulated with LPS to induce plasma cell differentiation *in vitro*. LPS is a structural component of the bacterial cell wall of many pathogens and induces B cell activation upon binding to the Toll-like receptor 4 (TLR4) (Murphy et al. 2007; see 1.1.). This leads to cell proliferation and differentiation of B cells into antibody-secreting plasmablast cells (Minguet et al., 2008).

CD43-depleted B cells from the secondary lymphoid organs, lymph nodes and spleen, of *Pax5*$^{S283A,T285A/S283A,T285A}$ mice and WT mice were stimulated *in vitro* with LPS for 4 days. Activated B cells (CD22^{+}), pre-plasmablast (CD22^{-} CD138^{-}) and plasmablast (CD22^{-} CD138^{+}) populations were examined by flow cytometry after 4 days of LPS stimulation (Figure 6A). No differences in the transition from activated B cells to plasmablasts could be detected in homozygous *Pax5*$^{S283A,T285A/S283A,T285A}$ B cells compared to *Pax5*$^{+/+}$ B cells (Figure 6A, B).

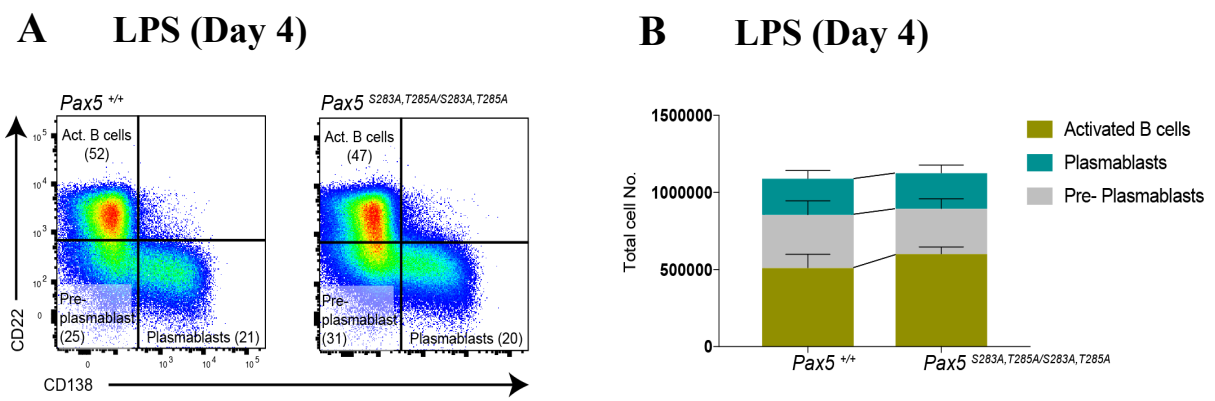

Figure 6. Normal activation of B cells upon lipopolysaccharide stimulation.
(A) *Pax5*$^{+/+}$ and *Pax5*$^{S283A,T285A/S283A,T285A}$ splenic B cells of age-matched mice were stimulated *in vitro* for 4 days with lipopolysaccharide (LPS) to induce B cell activation. Flow cytometric analysis of CD22^{+} activated B cells, CD22^{-} CD138^{-} pre-plasmablasts and CD138^{+} plasmablasts was performed. Representative FACS plots are shown. (B) Total cell numbers obtained from the flow cytometric analysis in (A) are shown with S.E.M. *Pax5*$^{+/+}$ n=3, *Pax5*$^{S283A,T285A/S283A,T285A}$ n=3. Similar data could be observed in two independent experiments.

Next, the LPS-induced antibody secretion and cell proliferation was examined. To address this, mature B cells were stained with CellTrace Violet^{TM} prior to LPS stimulation. CellTrace Violet^{TM} labels proteins and can therefore be used to analyze proliferation by measuring its dilution by subsequent flow cytometry. It has been shown that the immunoglobulin isotype IgG3 is produced upon LPS stimulation (Quintana et al., 2008). We therefore stained for IgG3^{+} cells in the CellTrace Violet^{TM}-treated mature B cells after 4 days of LPS stimulation and analyzed them by flow cytometry. Statistical analysis revealed a significant difference in IgG3 expressing cells in the *Pax5*$^{S283A,T285A/S283A,T285A}$ mutant B cells when compared to WT (Figure 7A,B). Moreover, the dilution of the CellTrace Violet ^{TM} reagent revealed that *Pax5*$^{S283A,T285A/S283A,T285A}$ B cells showed a delayed cell proliferation upon LPS stimulation (Figure 7C). *Pax5*$^{S283A,T285A/S283,T285A}$ B cells were delayed by one cycle of cell division when compared to the cell proliferation of *Pax5*$^{+/+}$ B cells and showed only 7 cell divisions, whereas WT B cells showed 8 cell divisions. It is clearly visible that *Pax5*$^{S283A,T285A/S283A,T285A}$ B cells had more cells residing in the first 6 cell cycles than WT (Figure 7C).

In addition to LPS stimulation, *Pax5*$^{S283A,T285A/S283A,T285A}$ mature B cells were also stimulated with LPS+IL4, CpG, IgM+IL4, αCD40+IL4 and BAFF+CD40L+IL4. However, no differences could be discovered regarding B cell activation, plasma cell differentiation and isotype switching of *Pax5*$^{S283A,T285A/S283A,T285A}$ mature B cells compared to WT mature B cells using these stimulation conditions (data not shown).

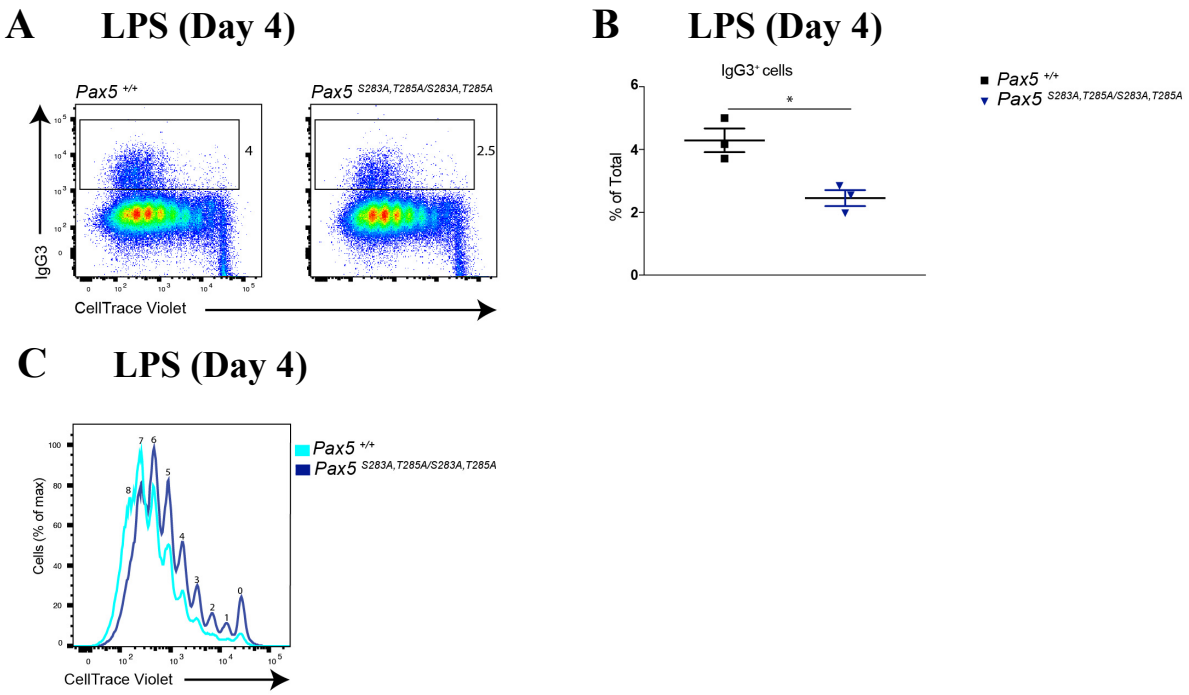

Figure 7. Decreased IgG3 CSR and delayed cell proliferation in *Pax5*$^{S283A,T285A/S283A,T285A}$ B cells upon LPS stimulation.
(A) Flow cytometric analysis of the indicated genotypes was performed on B cells stimulated with LPS for 4 days *in vitro*. Representative FACS plots are shown. (B) Statistical analysis of the relative percentage of IgG3$^+$ B cells shown in (A) were analyzed with mean ± S.E.M and Welch's t-test. Each symbols indicates the data of one mouse. *, $P < 0.05$. (C) Splenic B cells were stained with Celltrace Violet prior to 4 days LPS stimulation to reveal proliferation and cell division of the indicated genotypes. Numbers represent the number of cell divisions. Similar data was obtained in three independent experiments. *Pax5*$^{+/+}$ n=3, *Pax5*$^{S283A,T285A/S283A,T285A}$ n=3.

2.1.3 Normal Pax5-Blimp1 dynamics upon *in vitro* LPS stimulation

Previously, Yasuda et al. investigated the phosphorylation of Pax5 by ERK2. In this study, they identified ERK1/2 consensus sites in Pax5, including phosphorylation of S189, S284 and T285. However, experiments revealed ERK1/2- mediated phosphorylation of Pax5 at amino acids 189 and 283 *in vitro*. Furthermore, they claimed that the phosphorylation of these sites in *Pax5* leads to depression of Blimp1 which in turn initiates plasma cell differentiation (Yasuda et al., 2012).

To investigate Pax5-Blimp1 dynamics in *Pax5*$^{S283A,T285A/S283A,T285A}$ mice, splenic B cells of *Pax5*$^{S283A,T285A/S283A,T285A}$ and *Pax5*$^{+/+}$mice were stimulated with LPS *in vitro* and intracellular levels of Pax5 and Blimp1 were analyzed every day for 4 days. *Pax5* is expressed in activated B cell at high levels and then gradually declines until the plasmablast cell stage, in which Pax5 expression is completely abolished. Blimp1 on the other hand, behaves conversely

to Pax5, it starts to be expressed in pre-plasmablasts and reaches its expression peak in plasma cells (Kallies et al., 2007).

Pax5 and Blimp1 levels were measured in activated B cells, pre-plasmablasts and plasmablasts as defined in 2.1.2. The analysis showed no changes in the Pax5-Blimp1 expression dynamics in *Pax5*$^{S283A,T285A/S283A,T285A}$ B cells (Figure 8).

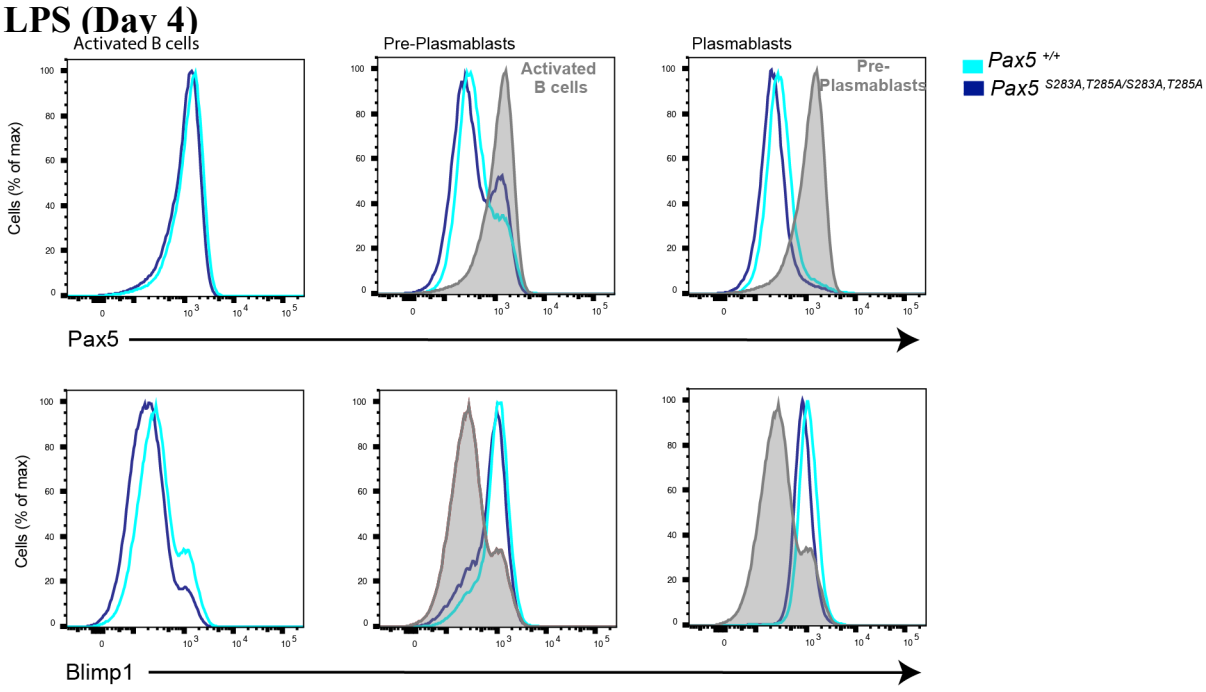

Figure 8. Normal Pax5-Blimp1 expression dynamics in *Pax5*$^{S283A,T285A/S283A,T285A}$ B cells. Splenic B cells of *Pax5*$^{+/+}$ and *Pax5*$^{S283A,T285A/S283A,T285A}$ mutant were stimulated for 4 days with LPS, and Pax5 and Blimp1 expression was monitored via intracellular staining followed by flow cytometric analysis. Representative histograms are shown. *Pax5*$^{+/+}$ n=4, *Pax5*$^{S283A,T285A/S283A,T285A}$ n=3.

2.1.4 Normal germinal center B cell and plasma cell differentiation in *Pax5*$^{S283A,T285A/S283A,T285A}$ mice upon NP-KLH immunization

Based on the findings in the LPS stimulation experiments of *Pax5*$^{S283A,T285A/S283A,T285A}$ B cells, *Pax5* mutant mice were challenged *in vivo* by immunizing them with the hapten 4-hydroxy-3-nitrophenyl acetyl (NP) coupled to the carrier protein keyhole limpet hemocyanin (KLH) in combination with the adjuvant alum. Immunization with NP-KLH results in a T cell-dependent B cell response and allowed us to investigate an NP-specific immune reaction.

Pax5$^{S283A,T285A/S283A,T285A}$ and *Pax5*$^{+/+}$ age-matched mice were immunized with NP-KLH. 14-days post immunization, GC B cells of lymph nodes and spleen were analyzed by flow cytometry. GC B cells were identified as GL7^{+}Fas^{+} cells. The analysis revealed no significant difference in GC B cell populations in the spleen and in lymph nodes of *Pax5*$^{S283A,T285A/S283A,T285A}$ mice compared to WT mice (Figure 9A, B).

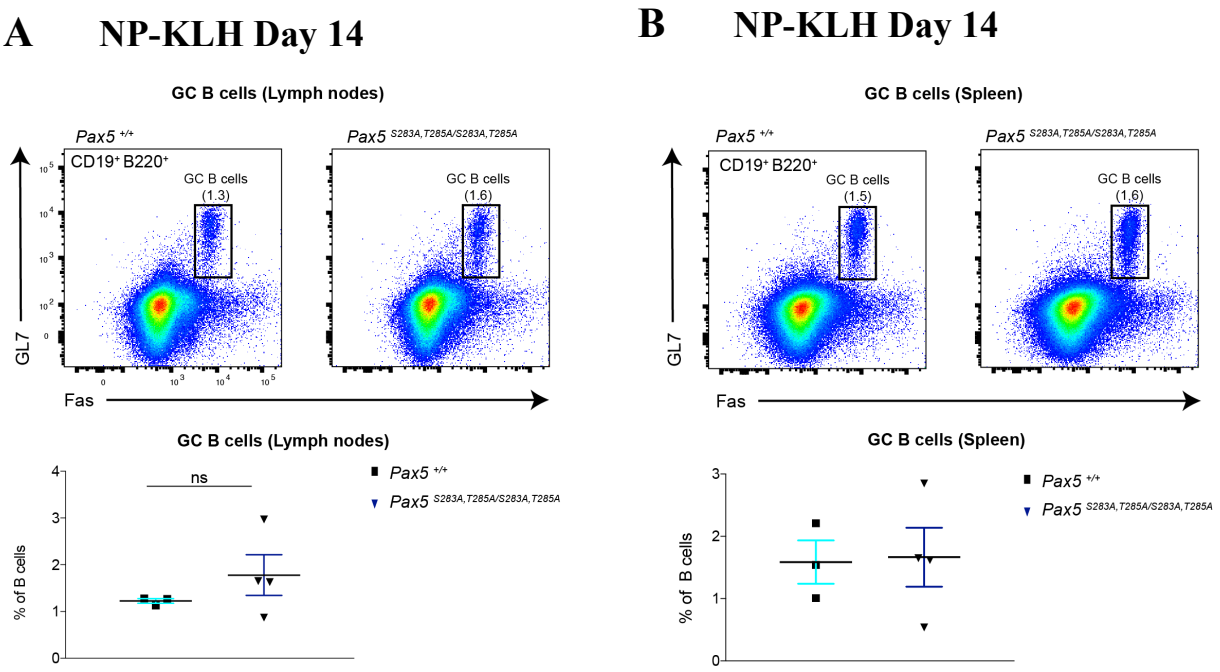

Figure 9. Normal germinal center B cell differentiation in *Pax5*$^{S283A,T285A/S283A,T285A}$ mice upon NP-KLH immunization.
(A, B) Age-matched mice of the indicated genotypes were immunized with hapten 4-hydroxy-3-nitrophenyl acetyl (NP) coupled to the carrier protein keyhole limpet hemocyanin (KLH). The lymph nodes (A) and spleen (B) were analyzed by flow cytometry 14-days post immunization. GL7^{+}Fas^{+} germinal center (GC) B cells shown in the FACS plots were statistically evaluated as relative percentage with mean ± S.E.M and Welch's t-test. Each symbol represents an individual mouse.

In addition, generation of NP-specific plasmablasts was investigated. Plasmablasts were identified as CD28^{+} CD138^{+} cells. However, no variation in the percentage of generated plasmablast in the lymph nodes or spleen could be detected in *Pax5*^{S283A,T285A,S283A,T285A} when compared to WT mice (Figure 10A, B).

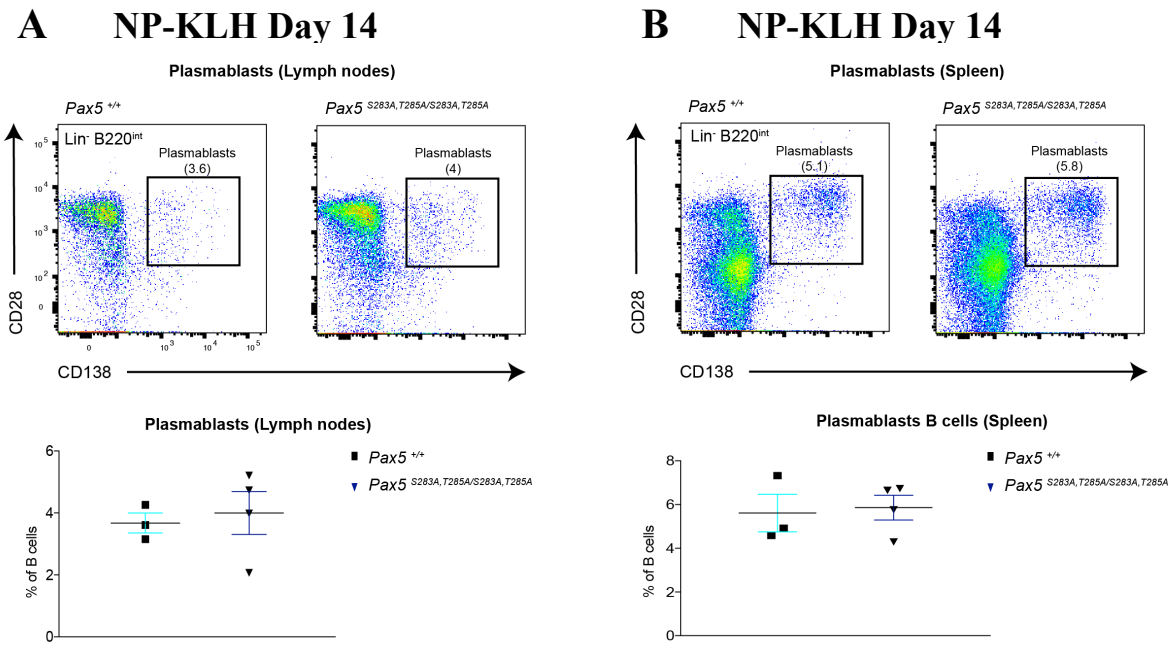

Figure 10. Normal differentiation into plasmablasts in *Pax5*$^{S283A,T285A/S283ATS285A}$ mice upon NP-KLH immunization.
(A) and (B) NP-KLH immunization of age matched mice of the indicated genotype. Flow cytometric analysis of lymph nodes (A) or spleen (B) have been performed 14-days after immunization. Statistical analysis of CD28^{+} CD138^{+} plasmablasts was performed with mean ± S.E.M.. Each symbol indicates an individual animal. Representative FACS plots are shown.

2.1.5 Decreased levels of IgG2b and IgM in the serum of *Pax5*$^{S283A,T285A/S283A,T285A}$ mice after NP-KLH immunization

Upon challenging the immune system with NP-KLH, high affinity antibodies of IgG2b and IgM isotypes are produced. Hence, the serum concentration of IgG2b and IgM was measured via Enzyme-linked Immunosorbent Assay (ELISA). *Pax5*$^{S283A,T285A/S283A,T285A}$ mice showed no significant reduction of NP-specific IgG2b and IgM levels compared to WT mice. However, a trend towards reduction was visible (Figure 11A, B).

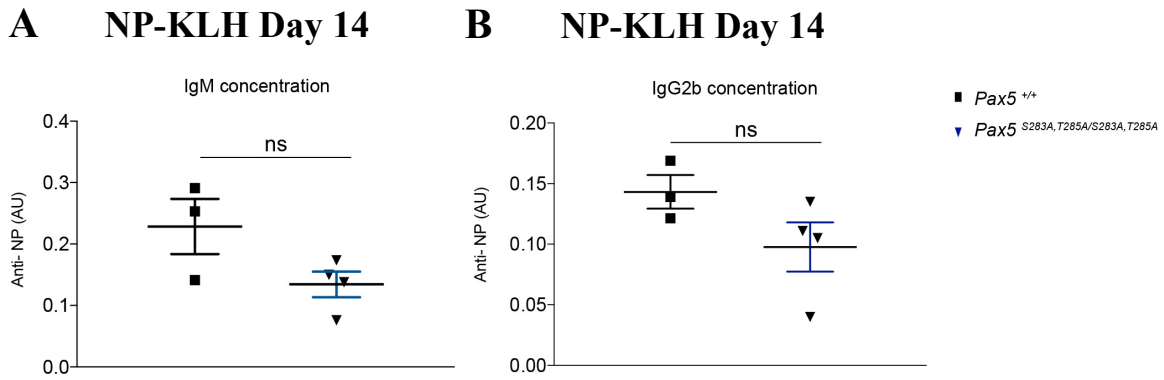

Figure 11. Decreased NP-specific antibody isotype concentration in the serum of *Pax5*$^{S283A,T285A/S283A,T285A}$ mice.
Serum was collected 14-days post NP-KLH immunization. NP-specific IgM (A) and IgG2b (B) concentration was determined via Enzyme-linked Immunosorbent Assay (ELISA). The concentration of the IgH isotypes is displayed as arbitrary unit (AU). Each symbol represents an individual mouse. Statistical analysis was performed with mean ± S.E.M. and Welch's t-test. (A) P=0.16. (B) P=0.13

2.2. Generation of the *Pax5*$^{\Delta HD}$ allele

In order to delete the partial homeodomain of Pax5, two sgRNAs, Cas9 mRNA and a repair template were injected into the cytoplasm of murine zygotes. The HD is located in exon 6 of *Pax5* and was deleted in frame (Figure 12A). Upon PCR amplification of the tail DNA of mice, a 349-bp WT fragment and 271-bp mutant fragment are generated (Figure 12B). In addition, the correctness of the mutation was verified by Sanger Sequencing (Figure 12C).

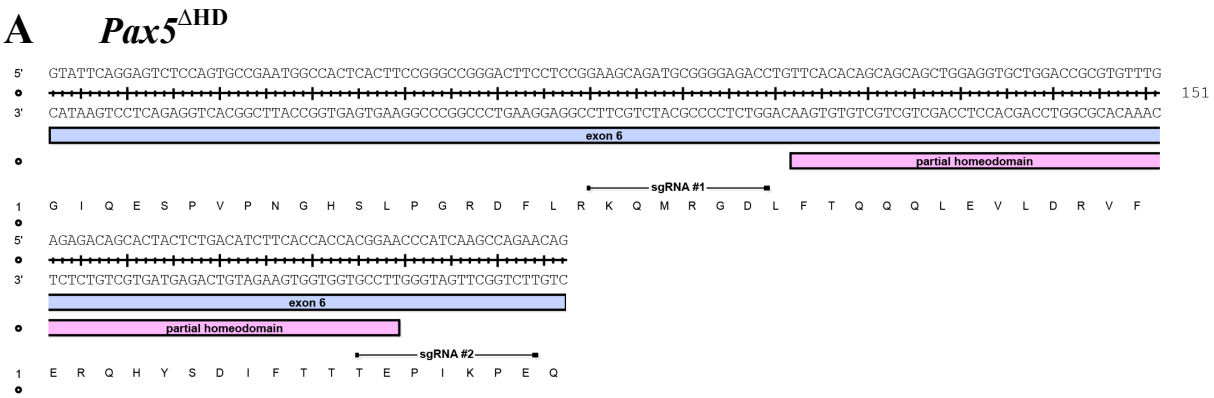

Figure 12. Generation of *Pax5*$^{\Delta HD}$allele.
(A) The sequence of exon 6 of *Pax5* is shown. The location of the partial homeodomain and the sequence of the single guide RNAs are displayed. (B) Gel electrophoresis picture of the genotyping of the *Pax5*$^{\Delta HD}$ allele. A 100-bp ruler was used as marker (M). Lane 1 shows the WT band at 349-bp and lane 2 shows *Pax5*$^{\Delta HD/+}$ with an additional 271-bp mutant fragment. (C) Sanger sequencing results of exon 6 of *Pax5*$^{\Delta HD}$ allele.

2.2.1. Normal B cell development in *Pax5*$^{\Delta HD/\Delta HD}$ mice in steady state

Analysis of the bone marrow, spleen and thymus revealed no difference in the presence of the B lymphocyte subsets as well as thymocytes in *Pax5*$^{\Delta HD/+}$ and *Pax5*$^{\Delta HD/\Delta HD}$ mice when compared to *Pax5*$^{+/+}$mice (Figure 13). However, *Pax5*$^{\Delta HD/\Delta HD}$ mature B cells in the bone marrow as well as in the spleen displayed slightly decreased levels of surface IgD (Figure 13B, D).

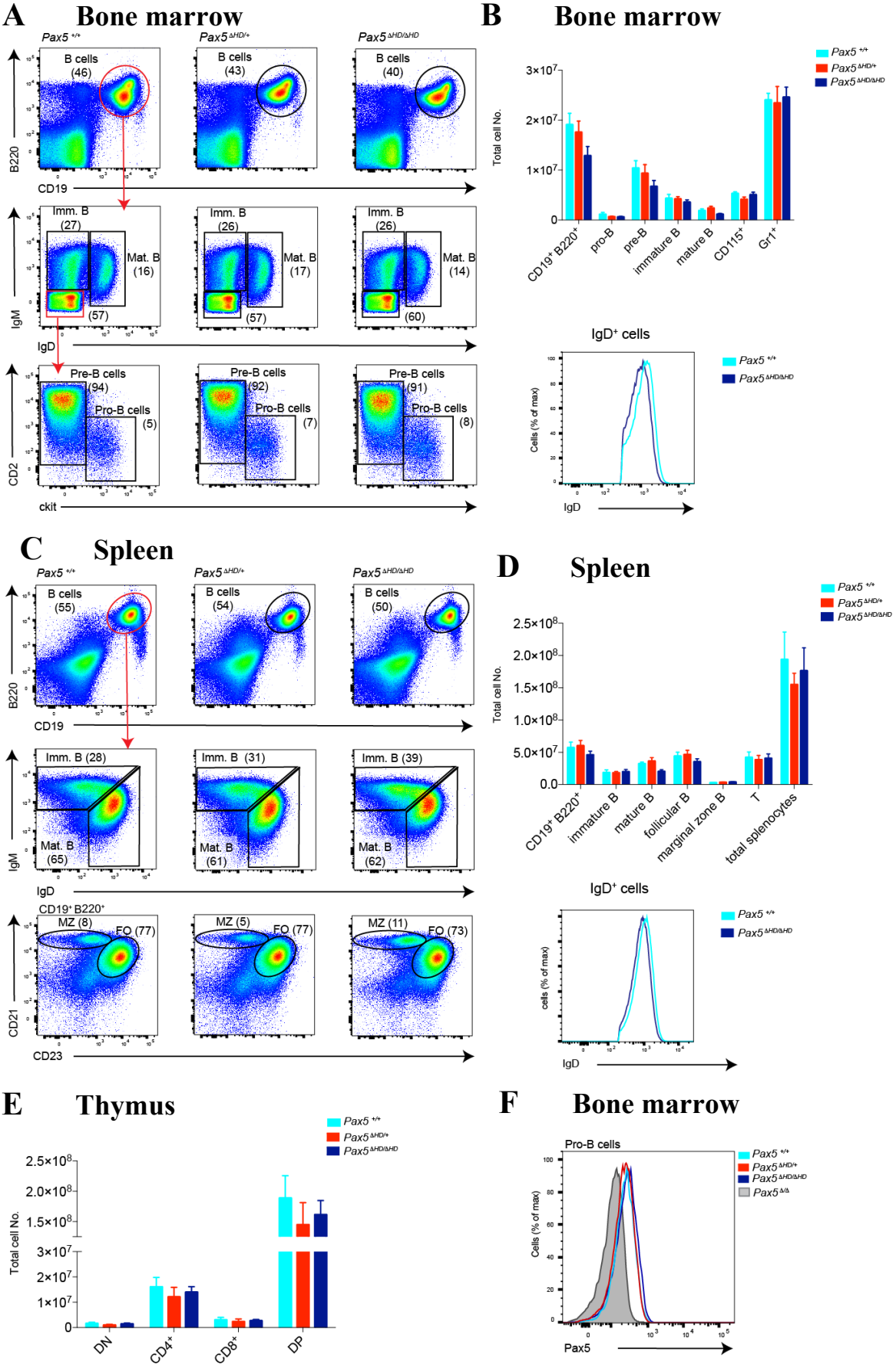
A
Bone marrow
Pax5 +/+
Pax5 ΔHD/+
Pax5 ΔHD/ΔHD
B cells (46)
B cells (43)
B cells (40)
B220
CD19
Imm. B (27)
Mat. B (16)
(57)
Imm. B (26)
Mat. B (17)
(57)
Imm. B (26)
Mat. B (14)
(60)
IgM
IgD
Pre-B cells (94)
Pro-B cells (5)
Pre-B cells (92)
Pro-B cells (7)
Pre-B cells (91)
Pro-B cells (8)
CD2
ckit
B
Bone marrow
Total cell No.
3×10^7
2×10^7
1×10^7
0
CD19+ B220+
pro-B
pre-B
immature B
mature B
CD115+
Gr1+
IgD+ cells
Cells (% of max)
IgD
C
Spleen
B cells (55)
B cells (54)
B cells (50)
Imm. B (28)
Mat. B (65)
Imm. B (31)
Mat. B (61)
Imm. B (39)
Mat. B (62)
CD19+ B220+
MZ (8)
FO (77)
MZ (5)
FO (77)
MZ (11)
FO (73)
CD21
CD23
D
Spleen
2.5×10^8
2.0×10^8
1.5×10^8
1.0×10^8
5.0×10^7
0.0
CD19+ B220+
immature B
mature B
follicular B
marginal zone B
T
total splenocytes
E
Thymus
2.5×10^8
2.0×10^8
1.5×10^8
3×10^7
2×10^7
1×10^7
0
DN
CD4+
CD8+
DP
F
Bone marrow
Pro-B cells
Pax5 Δ/Δ
Pax5

Figure 13. Normal B cell development in *Pax5*$^{\Delta HD/\Delta HD}$ mice.
(A-B) Flow cytometric analysis of BM of the indicated genotypes. For the analysis, 4-8 week-old littermates were investigated. Statistical analysis of total BM cell numbers was performed with mean ± S.E.M.. Surface IgD levels of *Pax5*$^{\Delta HD/\Delta HD}$ mature B cells were compared to *Pax5*$^{+/+}$ mature B cells. Representative FACS plots and histograms are shown. (C-D) B cell development and total cell numbers of splenocytes. Statistical analysis was performed as described in (B). (E) Total cell numbers of thymus of the indicated genotypes. (F) Intracellular Pax5 staining of pro-B cells of the indicated genotypes. A monoclonal rabbit anti-PAx5 antibody was used which was subsequently detected via an anti-rabbit APC FACS antibody. *Pax5*$^{+/+}$ n=5, *Pax5*$^{\Delta HD/+}$ n=4, *Pax5*$^{\Delta HD/\Delta HD}$ n=5

2.2.2. Increased plasmablast numbers in *Pax5*$^{\Delta HD/\Delta HD}$ mice upon LPS stimulation

To address whether the deletion of the partial homeodomain of Pax5 has an effect on B cell activation, WT and *Pax5*$^{\Delta HD/\Delta HD}$ mature B lymphocytes were stimulated with LPS as stated in 2.1.2.

Flow cytometric analysis revealed that *Pax5*$^{\Delta HD/\Delta HD}$ B cells gave rise to lower numbers of activated B cells but show higher percentage of plasmablasts when compared to *Pax5*$^{+/+}$ B cells (Figure 14A, B).

Additionally, LPS+IL4, CpG, IgM+IL4, αCD40+IL4 and BAFF+CD40L+IL4 stimulations were performed with *Pax5*$^{\Delta HD/\Delta HD}$ mature B cells. However, these did not reveal any significant differences when compared to WT mature B cells (data not shown).

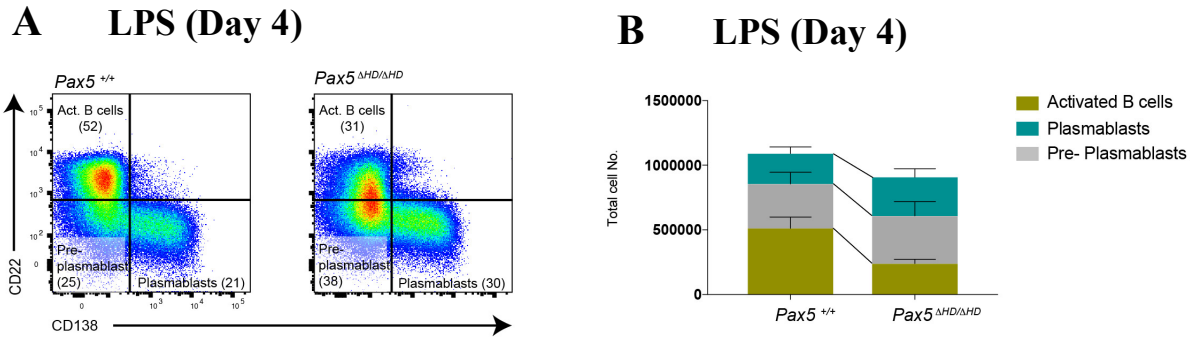

Figure 14. Increased plasma cell differentiation in *Pax5*$^{\Delta HD/\Delta HD}$ mature B cells *in vitro*.
(A) Splenic B cells of the indicated genotypes were stimulated with LPS for 4 days. The stimulation experiment was performed with B cells from age-matched mice. CD22^{+} activated B cells, CD22^{-}CD138^{-} pre-plasmablasts and CD138^{+} plasmablasts were analyzed by flow cytometry. Representative FACS plots are shown. (B) Statistical analysis of total cell numbers with mean ± S.E.M.. *Pax5*$^{+/+}$ n=3, *Pax5*$^{\Delta HD/\Delta HD}$ n=3. Similar data was generated in two different experiments.

2.2.3. Decreased switching to IgG3 and delayed cell proliferation in *Pax5*$^{\Delta HD/\Delta HD}$ mature B cells upon LPS stimulation

As specified in 2.1.2., *Pax5*$^{\Delta HD}$ B lymphocytes were stained with CellTrace Violet^{TM} prior to 4 days of LPS stimulation to investigate cell proliferation *in vitro*.

First, switching to IgG3 was examined in *Pax5*$^{\Delta HD/\Delta HD}$ mature B cells. Analysis of the relative percentage of IgG3^{+} cells in *Pax5*$^{\Delta HD/\Delta HD}$ mature B cells compared to WT mature B cells showed a trend towards reduction of IgG3 expression. However, statistical analysis revealed no significant reduction of IgG3 in *Pax5*$^{\Delta HD/\Delta HD}$ mature B cells (Figure 15A, B).

Second, the cell proliferation of *Pax5*$^{\Delta HD/\Delta HD}$ B cells compared to *Pax5*$^{+/+}$ B cells was addressed. Upon LPS stimulation, delayed cell proliferation by one cell cycle could be identified in *Pax5*$^{\Delta HD/\Delta HD}$ B cells. Whereas *Pax5*$^{+/+}$ B cells displayed 8 completed cell cycles, *Pax5*$^{\Delta HD/\Delta HD}$ B cells only showed 7 cell cycles. Additionally, more *Pax5* *Pax5*$^{\Delta HD/\Delta HD}$ B cells resided in the first 6 cell cycles (Figure 15C).

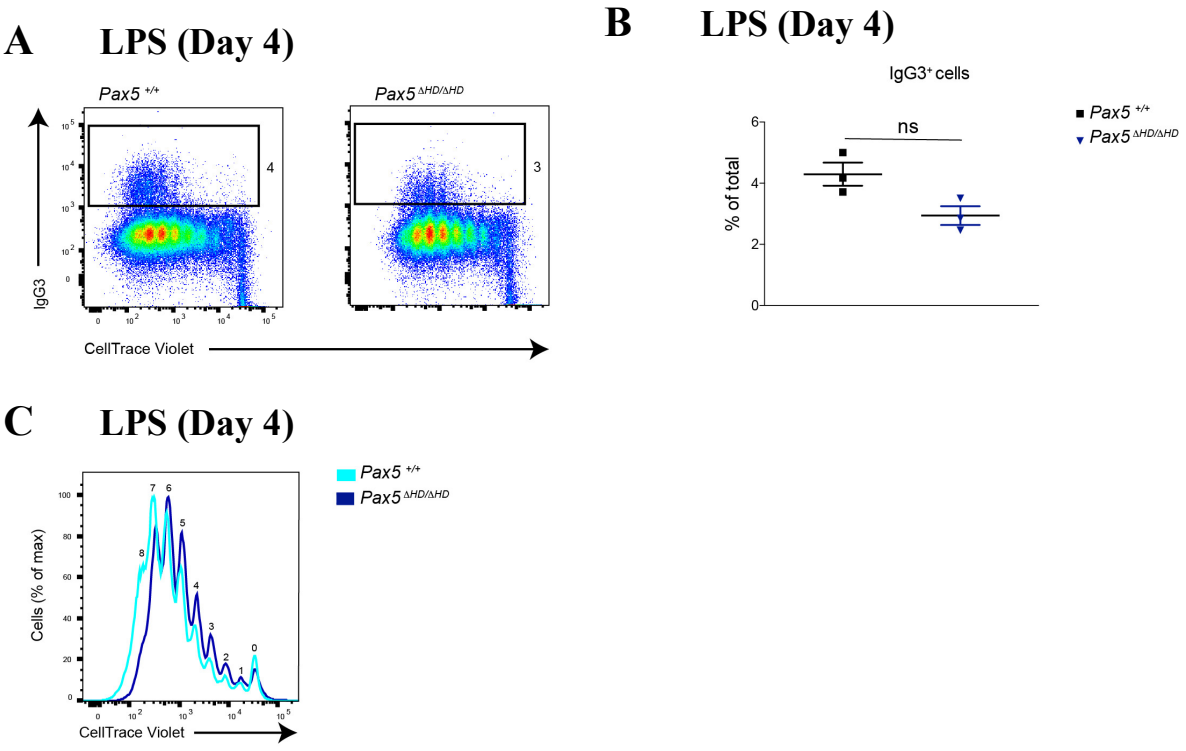

Figure 15. Decreased IgG3 CSR and delayed cell proliferation in *Pax5*$^{\Delta HD/\Delta HD}$ B cells upon LPS stimulation.
(A) Splenic B cells of age-matched *Pax5*$^{+/+}$ and *Pax5*$^{\Delta HD/\Delta HD}$ mice were stimulated with LPS for 4 days followed by flow cytometric analysis to examine IgG3 expression. Representative FACS plots are shown. (B) Statistical analysis of the relative percentage of IgG3^{+} B cells displayed in (A) were performed with mean ± S.E.M and Welch's t-test. Each symbol represents one animal. P= 0.052. (C) Celltrace Violet was administered to splenic B cells prior to 4 days of LPS stimulation to determine cell proliferation and cell division of *Pax5*$^{+/+}$ B cells and *Pax5*$^{\Delta HD/\Delta HD}$ B cells. Numbers indicate the amount of cell division of the stimulated cells. A representative histogram is shown. Similar data was obtained in three independent experiments.

2.2.4. Unaltered Pax5-Blimp1 dynamics in *in vitro* LPS-stimulated *Pax5*$^{\Delta HD/\Delta HD}$ mature B cells

Pax5 and Blimp1 expression is mutually exclusive (see 1.4.3). Since Blimp1 is the master regulator of plasma cells (Murphy et al. 2007), we hypothesized that Pax5-Blimp1 expression dynamics might be altered and could thus cause the accumulation of plasmablasts shown in 2.2.2.

The expression of Pax5 and Blimp1 was analyzed over the course of 4 days of LPS stimulation in *Pax5*$^{\Delta HD/\Delta HD}$ mature B cells as it is stated in 2.1.2. Activated B cells, pre-plasmablasts and plasmablasts were examined by flow cytometry. However, no difference in the expression levels of Pax5 and Blimp1 could be detected at the various stages of plasma cell differentiation between *Pax5*$^{\Delta HD/\Delta HD}$ and WT cells (Figure 16).

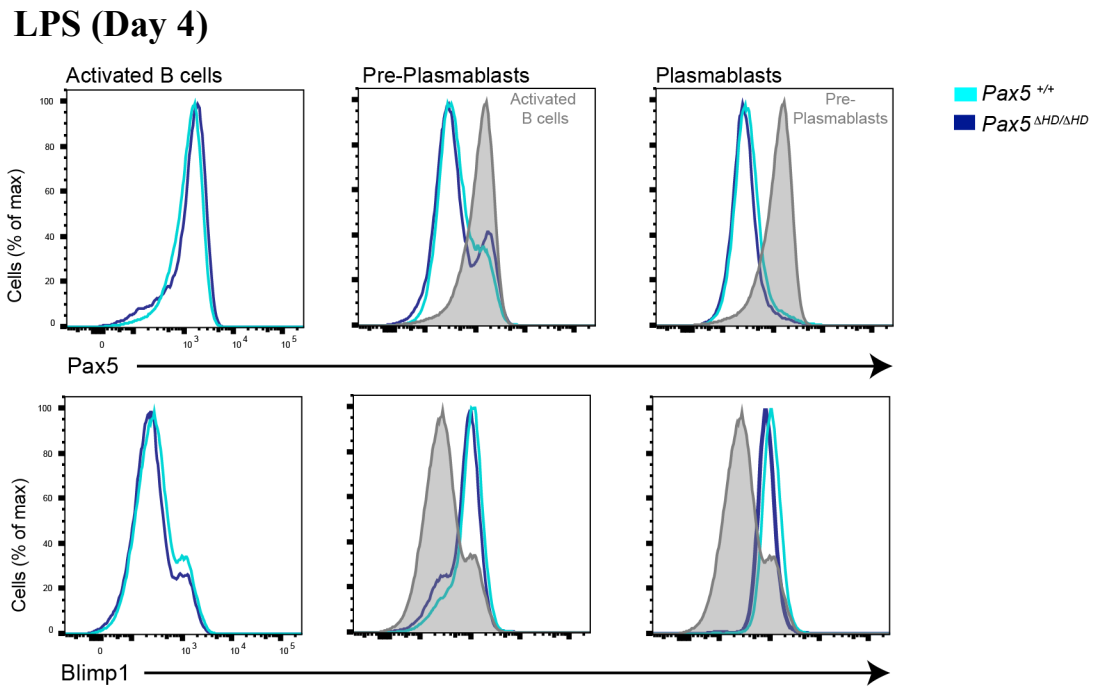

Figure 16. No altered dynamics between Pax5 and Blimp1 expression in the *Pax5*$^{\Delta HD/\Delta HD}$ mutant.
Splenocytes of indicated genotypes were stimulated with LPS for 4 days. Intracellular Pax5 and Blimp1 expression was investigated via flow cytometry analysis. Histogram graphs of representative experiments are shown. *Pax5*$^{+/+}$ n=3, *Pax5*$^{\Delta HD/\Delta HD}$ n=3

2.2.5. Decreased GC B cell population and increased plasmablast population in *Pax5*$^{\Delta HD/\Delta HD}$ mice upon NP-KLH immunization

Since *Pax5*$^{\Delta HD/\Delta HD}$ B cells showed a trend towards decreased switching to IgG3 and higher amounts of plasmablasts in *in vitro* LPS stimulation experiments, GC B cells and plasmablasts were analyzed upon challenging the mice with NP-KLH. The experiment was performed as described in 2.1.4.

Interestingly, significantly decreased amounts of GC B cells could be identified in the spleen of *Pax5*$^{\Delta HD/\Delta HD}$ mice (Figure 17A). The GC B cells in the lymph nodes also displayed a reduced percentage of GC B cells, however the difference was not significant when statistical analysis was applied (Figure 17B).

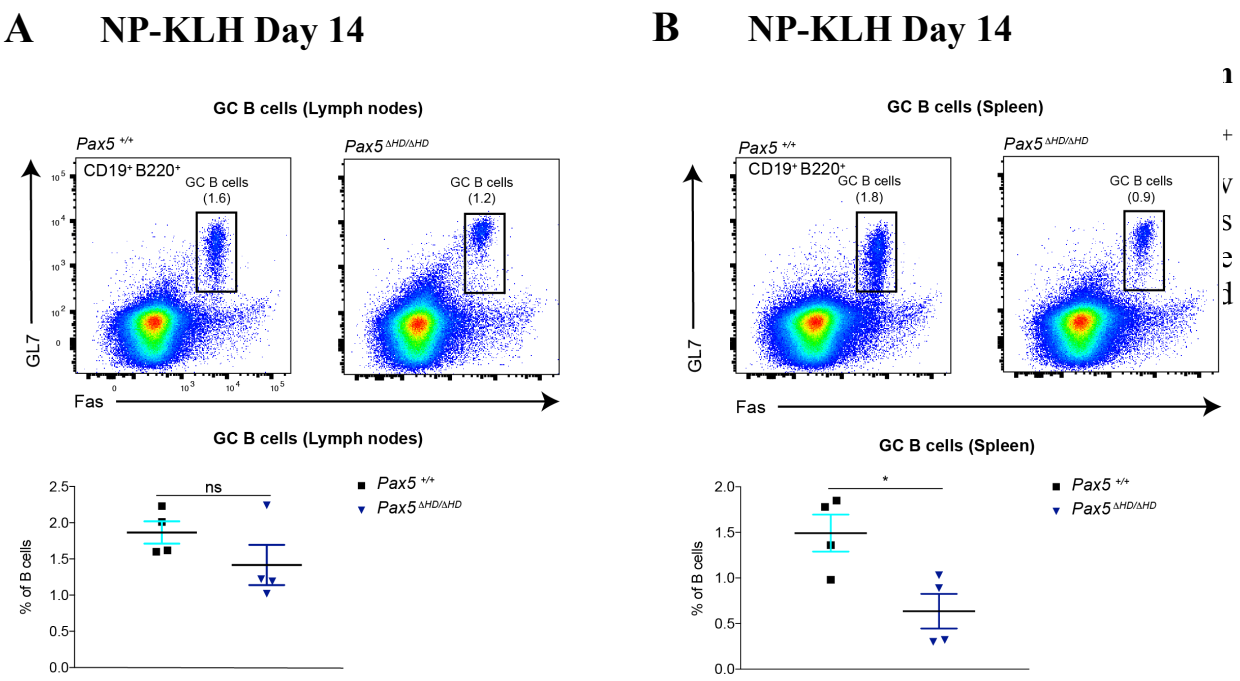

In line with the *in vitro* data, *Pax5*$^{\Delta HD/\Delta HD}$ mice showed increased plasmablasts cell populations in the lymph nodes and spleen compared to WT mice (Figure 18A, B).

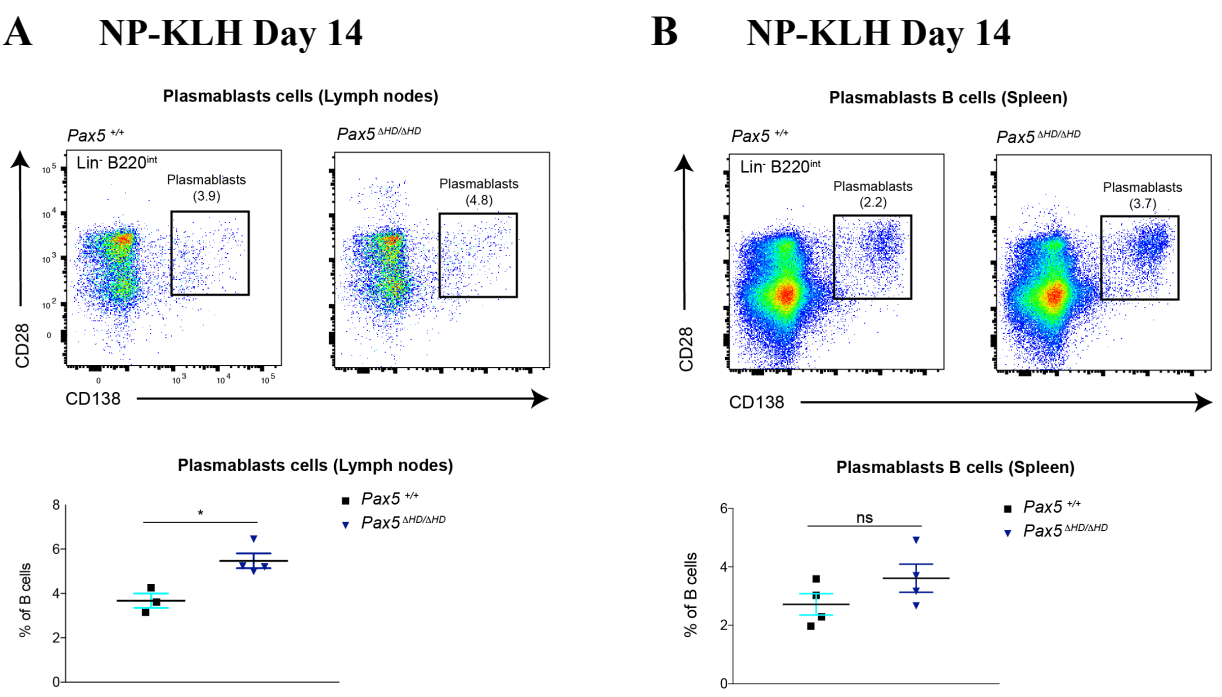

Figure 18. Increased numbers of plasmablasts in *Pax5*$^{\Delta HD/\Delta HD}$ mice upon NP-KLH immunization.
CD28^{+} CD138^{+} plasmablasts from lymph nodes (A) or spleen (B) of age-matched *Pax5*$^{+/+}$ and *Pax5*$^{\Delta HD/\Delta HD}$ mice were analyzed 14-days post NP-KLH immunization. Relative percentages of plasmablasts, shown in the FACS plots, were examined via statistical analysis with mean ± S.E.M. and Welch's t-test. Each symbols indicates data from one mouse. *, $P < 0.05$. Representative FACS plots are shown. Similar results have been generated in two independent experiments.

2.2.6. Lower concentration of IgG2b and IgM in the sera of immunized *Pax5*$^{\Delta HD/\Delta HD}$ mice

To address whether *Pax5*$^{\Delta HD/\Delta HD}$ mice show reduced Ig isotype switching *in vivo*, the sera of NP-KLH immunized *Pax5*$^{\Delta HD/\Delta HD}$ mice were analyzed for NP-specific IgG2b and anti-NP IgM via ELISA.

In correlation with the *in vitro* data, lower concentration of NP-specific IgG2b and IgM could be identified in *Pax5*$^{\Delta HD/\Delta HD}$ mice compared to WT mice. However, statistical analysis revealed only a significant reduction for IgG2b switching (Figure 19A, B).

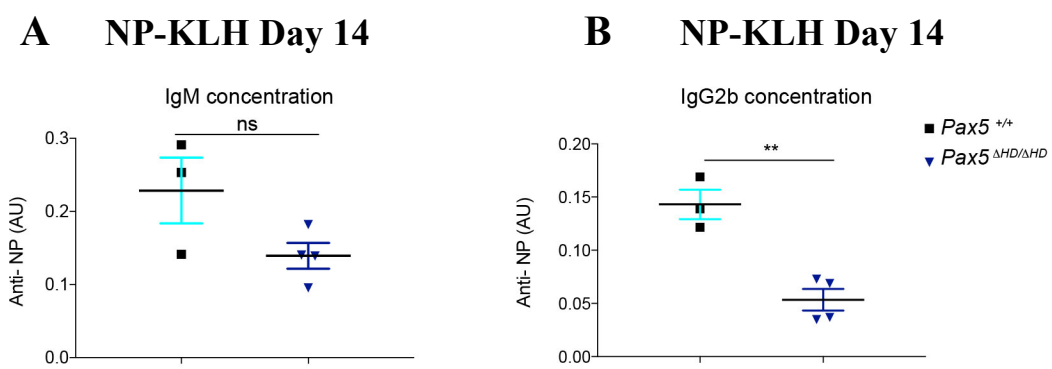

Figure 19. Decreased concentration of NP-specific IgM and IgG2b in the serum of *Pax5*$^{\Delta HD/\Delta HD}$ mice.

(A-B) Age-matched mice were immunized with NP-KLH. The serum was collected 14-days post immunization, and the concentration of NP-specific IgM (A) and IgG2b (B) was measured via ELISA. Each symbol represents an individual animal. Statistical analysis was performed with mean ± S.E.M. and Welch's t-test. **, $P < 0.01$.

2.3. Generation of the *Pax5*$^{\Delta TAD}$ allele

For the generation of *Pax5*$^{\Delta TAD}$ allele, a frameshift mutation was introduced by deleting one guanine nucleotide in exon 8 of *Pax5*. This led to a frameshift after 2 amino acids of the Pax5 TAD resulting in a truncated Pax5 protein after 6 amino acids (Figure 20A). The mutation of the PAM sequence (see 2.1.) generated the restriction site ClaI in the *Pax5*$^{\Delta TAD}$ allele. For genotyping of the TAD mutant mice, a 490-bp WT fragment and a 301-bp and a 189-bp mutant fragment can be detected by gel electrophoresis after PCR and restriction digest (Figure 20B). In addition, the correctness of the mutation was verified by Sanger Sequencing (Figure 20C).

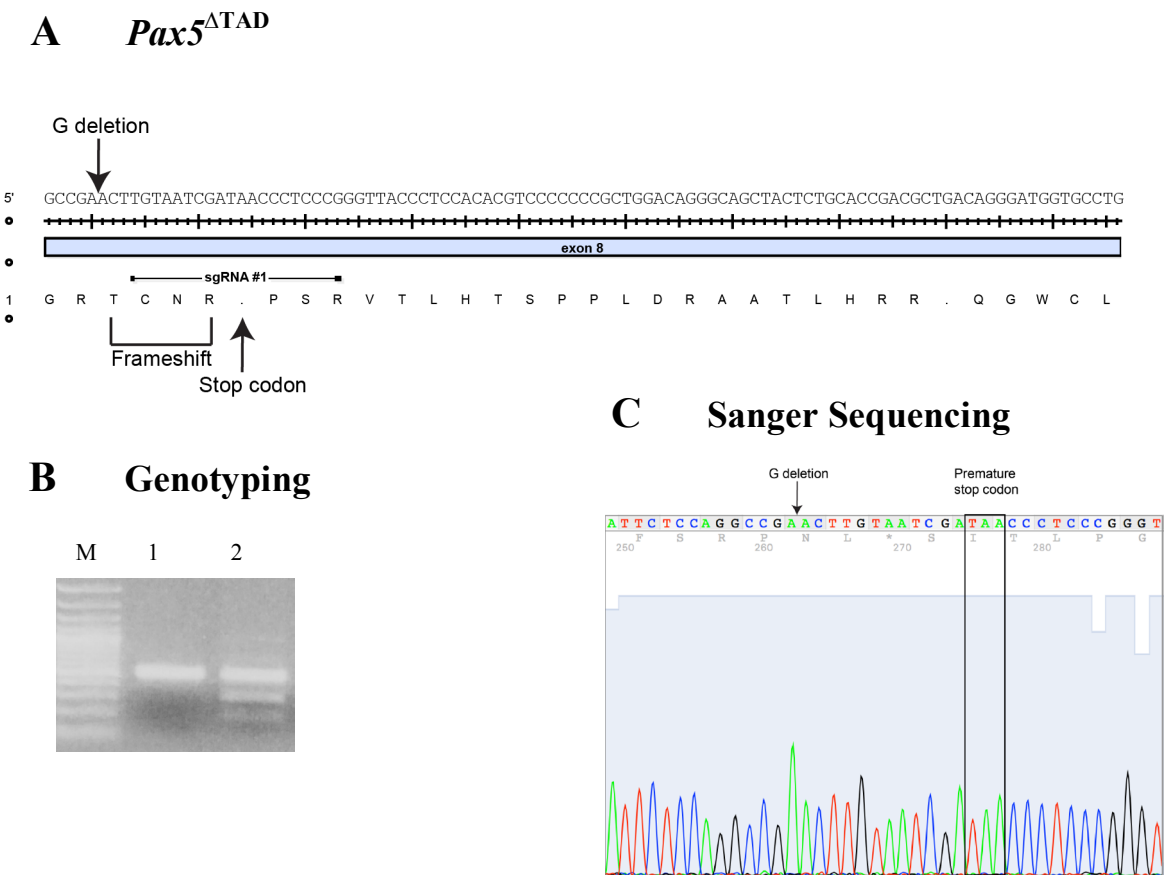

Figure 20. Generation of the *Pax5*$^{\Delta TAD}$ allele.
(A) Sequence of *Pax5*$^{\Delta TAD}$ mutant displaying the deleted guanine and the premature stop codon in the beginning of exon 8 of *Pax5*. (B) Gel electrophoresis picture of genotyping of *Pax5*$^{\Delta TAD}$ mutant mice after PCR amplification and *ClaI* digest. Lane 1 displays the 490-bp WT fragment. In lane 2, the mutant bands of a *Pax5*$^{\Delta TAD/+}$ mouse at 301-bp and 289-bp are visible. 100-bp ruler was used as M. (C) Sanger sequencing of *Pax5*$^{\Delta TAD}$allele verifying the deletion of guanine and the generation of the premature stop codon.

2.3.1. Developmental block at the pre-pro-B cell stage in *Pax5*$^{\Delta TAD/\Delta TAD}$ mice

Homozygous *Pax5*$^{\Delta TAD/\Delta TAD}$ mice exhibited a severe growth retardation and died at weaning age (data not shown). In addition, *Pax5*$^{\Delta TAD/\Delta TAD}$ mice did not display CD19^{+} B cells in the bone marrow (Figure 21A). Accordingly, all B cell cell subset in the bone marrow were absent. Nevertheless, B lymphopoiesis of heterozygous *Pax5*$^{\Delta TAD/+}$ mice did not show any impairment compared to WT mice (Figure 21A, B).

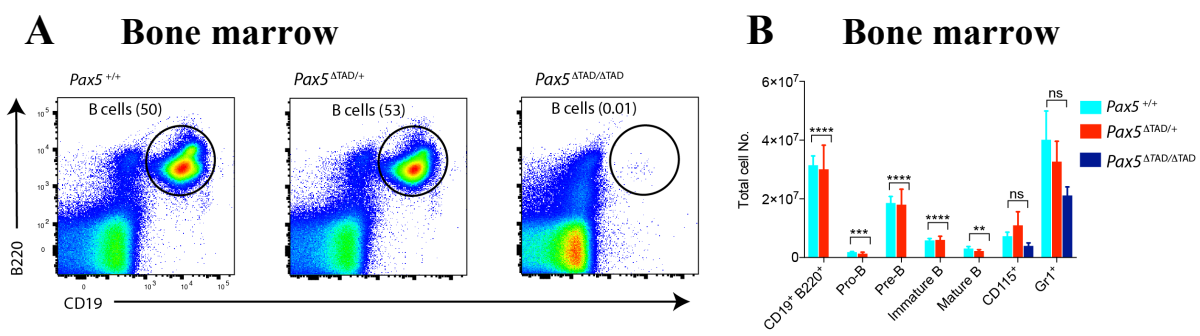

Figure 21. Developmental block of B lymphopoiesis in *Pax5*$^{\Delta TAD/\Delta TAD}$ mice.
(A) Flow cytometric analysis of BM of the indicated genotypes. For the analysis 2.5-week-old littermates were analyzed. Representative FACS plots are shown. (B) Statistical analysis of total cell numbers with mean ± S.E.M. and Welch's t-test. *, $P < 0.05$; **, $P < 0.01$; ***, $P < 0.001$; ****, $P < 0.0001$. *Pax5*$^{+/+}$ n=8, *Pax5*$^{\Delta TAD/+}$ n=6, *Pax5*$^{\Delta TAD/\Delta TAD}$ n=5.

To characterize the B cell developmental block in *Pax5*$^{\Delta TAD/\Delta TAD}$ mice more precisely, cells extracted from the BM of 3-week-old mice were analyzed by flow cytometry using markers expressed in B cell progenitors. As a control, *Pax5*$^{\Delta/\Delta}$ mice and *Pax5*$^{+/-}$ mice were included in the analysis. The flow cytometric analysis revealed that *Pax5*$^{\Delta TAD/\Delta TAD}$ cells are blocked at the pre-pro B-cell stage (Figure 22). The expression of the surface markers B220^{+} Ly6D^{+} c-Kit^{+} Flt3^{+} and Il7Rα^{+} has been previously described as markers for the identification of pre-pro-B cells (Inlay et al. 2009).

Bone marrow

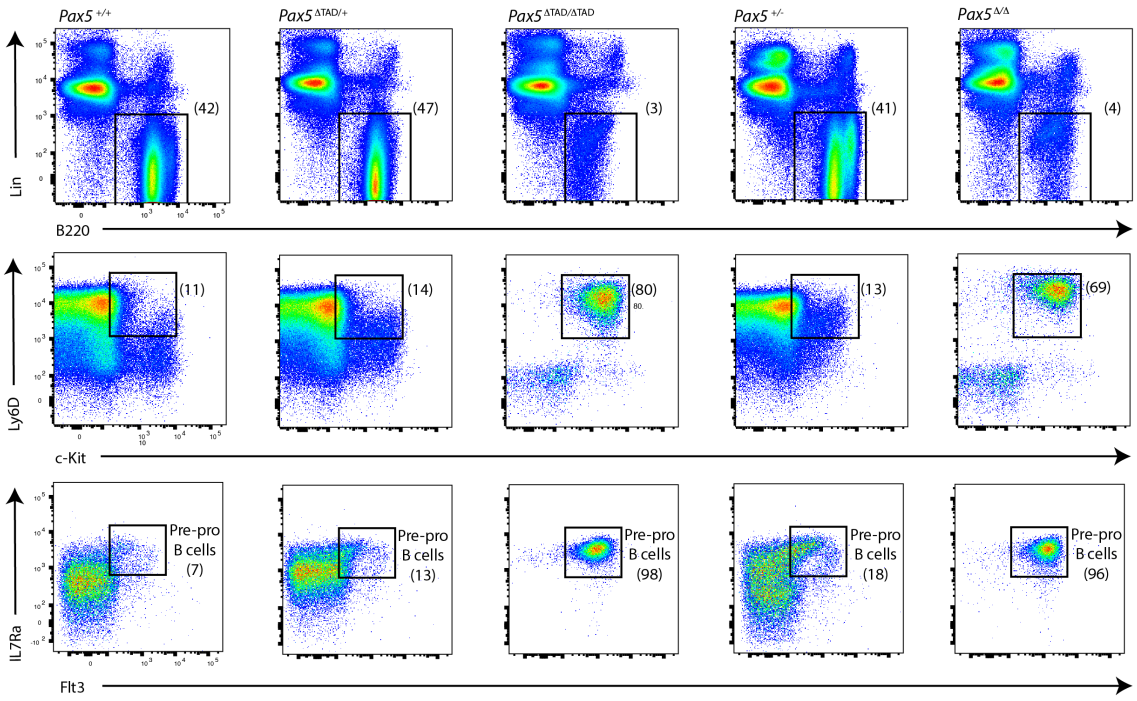

Figure 22. Arrest of *Pax5*$^{\Delta TAD/\Delta TAD}$ B cells in the pre-pro-B cell stage.
Flow cytometric analysis of the BM of 3-week-old littermates (*Pax5*$^{+/+}$mice, *Pax5*$^{\Delta TAD/+}$mice, *Pax5*$^{\Delta TAD/\Delta TAD}$ mice). *Pax5*$^{+/-}$ mice and *Pax5*$^{\Delta/\Delta}$ mice are age-matched. Lineage staining (Lin): CD3, CD4, CD8, CD11b, DX5, Gr1, Ly6C, Ter119 and NK1.1. Representative FACS plots are shown. *Pax5*$^{+/+}$ n=1, *Pax5*$^{\Delta TAD/+}$ n=2, *Pax5*$^{\Delta TAD/\Delta TAD}$ n=3, *Pax5*$^{+/-}$ n=1, *Pax5*$^{\Delta/\Delta}$ n=1.

2.3.2. Absence of splenic B cells in *Pax5*$^{\Delta TAD/\Delta TAD}$ mice

In line with the results of the flow cytometric analysis of the bone marrow, no B cells were present in the spleen of *Pax5*$^{\Delta TAD/\Delta TAD}$ mice (Figure 23A, B). Furthermore, *Pax5*$^{\Delta TAD/\Delta TAD}$ mice showed a severely reduced spleen size (Figure 23C). However, T cell populations in the spleen and thymus were present in *Pax5*$^{\Delta TAD/\Delta TAD}$ mice (Figure 23A, B, D, E).

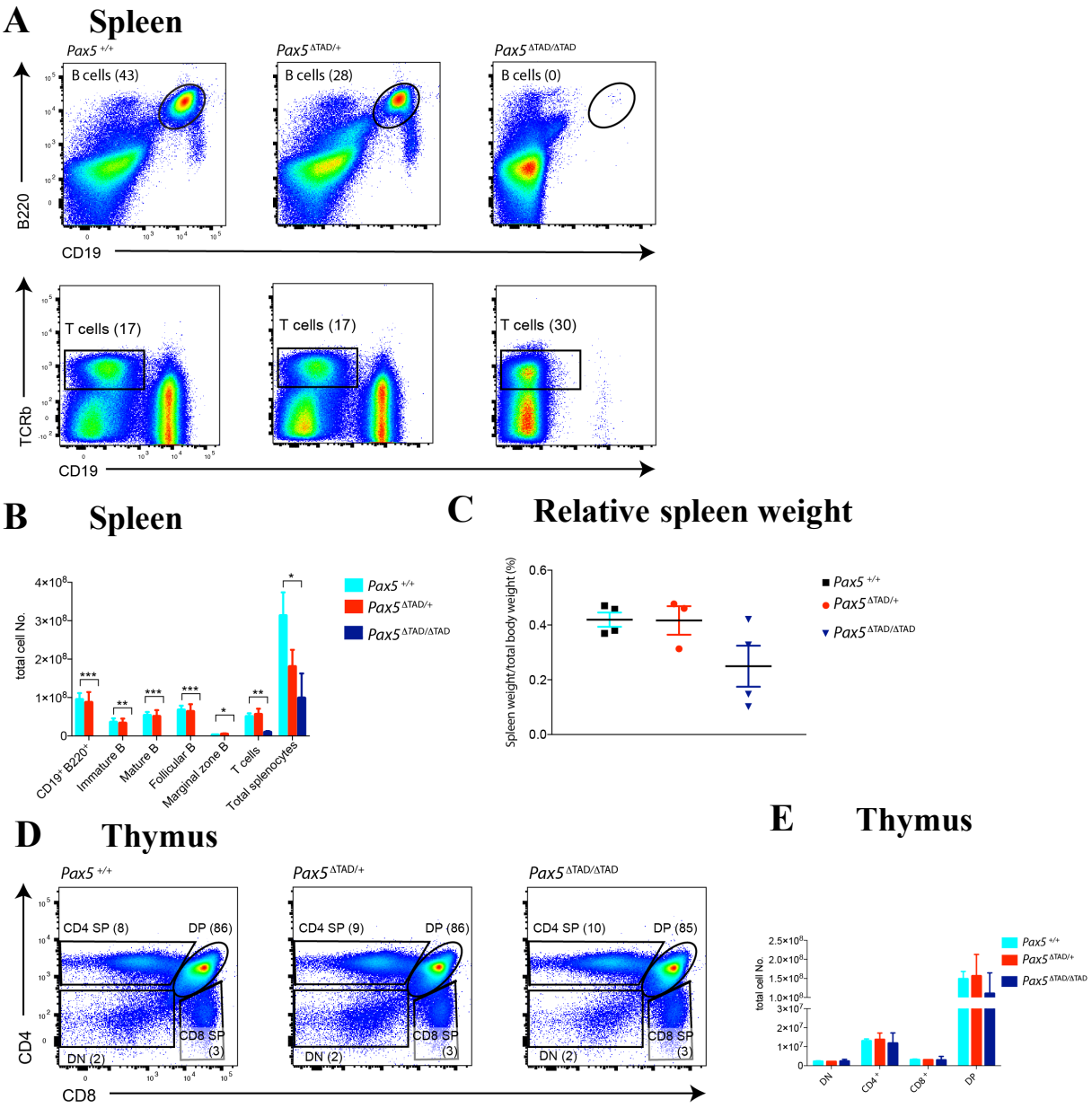

Figure 23. Absence of B cells in the spleen of *Pax5*$^{\Delta TAD/\Delta TAD}$ mice.
(A) Splenocytes of 3-week-old littermates of the indicated phenotype were analyzed via flow cytometric analysis. Representative FACS plots are shown. (B) Total cell numbers with statistical measurements with mean ± S.E.M. and Welch's t-test. *, $P < 0.05$; **, $P < 0.01$; ***, $P < 0.001$. *Pax5*$^{+/+}$ n=6, *Pax5*$^{\Delta TAD/+}$n=4, *Pax5*$^{\Delta TAD/\Delta TAD}$ n=5 (C) Relative spleen weight of the indicated genotypes. Each symbol represents an individual mouse. (D) Thymocytes were analyzed of 6-week-old littermates via flow cytometry of the indicated genotypes. Representative FACS plots are shown (E) Statistical analysis of cell numbers in (D) was performed with mean ± S.E.M.. *Pax5*$^{+/+}$ n=4, *Pax5*$^{\Delta TAD/+}$n=2, *Pax5*$^{\Delta TAD/\Delta TAD}$ n=3.

2.3.3. Pax5 expression in *Pax5*$^{\Delta TAD/\Delta TAD}$ mice

To determine whether the expression of the truncated Pax5 protein is stable or is not affected by nonsense-mediated mRNA decay, *ex vivo* intracellular Pax5 levels were investigated by flow cytometry. Age-matched *Pax5*$^{\Delta/\Delta}$ and *Pax5*$^{+/-}$ mice were included in the analysis in order to identify and compare different levels of Pax5 expression to that of *Pax5*$^{\Delta TAD/\Delta TAD}$ cells. Pax5 protein levels were measured in Lin^{-} B220^{+} c-Kit^{+} Ly6D^{+} cells. *Pax5*$^{\Delta TAD/+}$ B cells showed intermediate Pax5 levels when compared to WT and *Pax5*$^{\Delta TAD/\Delta TAD}$ B cells. However, *Pax5*$^{\Delta TAD/\Delta TAD}$ B cells showed increased Pax5 protein levels compared to *Pax5*$^{\Delta/\Delta}$ and *Pax5*$^{+/-}$ B cells (Figure 24A).

In addition, cells were extracted from the bone marrow of 3-week-old mice and CD19-enriched (for *Pax5*$^{+/+}$cells, *Pax5*$^{\Delta TAD/+}$ cells) and B220-enriched (for *Pax5*$^{\Delta TAD/\Delta TAD}$ cells, *Pax5*$^{+/-}$ cells, *Pax5*$^{\Delta/\Delta}$ cells) cells were taken in culture for *in vitro* expansion. A difference in growth behavior could be monitored since *Pax5*$^{\Delta TAD/\Delta TAD}$ cells required approximately 2-fold as long as *Pax5*$^{+/+}$ and *Pax5*$^{\Delta TAD/+}$ cells to reach the same density on a 15cm cell culture dish (data not shown). The *in vitro* expanded cells were subsequently used for flow cytometric analysis of intracellular Pax5 levels and for the generation of nuclear extracts. The nuclear extracts of *Pax5*$^{+/+}$, *Pax5*$^{\Delta TAD/+}$, *Pax5*$^{\Delta TAD/\Delta TAD}$ and *Pax5*$^{\Delta/\Delta}$ B cells were used for western blotting. The band at 36 kDa resembled the truncated Pax5 protein in *Pax5*$^{\Delta TAD/\Delta TAD}$ B cells and showed similar intensity as the 42 kDa WT Pax5 band. Nevertheless, the WT Pax5 band displayed a greater intensity than the truncated Pax5 protein in heterozygous *Pax5*$^{\Delta TAD/+}$ B cells. (Figure 24B).

Flow cytometric analysis of the *in vitro* cultured B cells revealed different Pax5 expression profiles for *Pax5*$^{\Delta TAD/\Delta TAD}$ B cells and *Pax5*$^{+/-}$ B cells than it has been observed *ex vivo.* When compared to *Pax5*$^{+/-}$ B cells, *Pax5*$^{\Delta TAD/\Delta TAD}$ B cells showed lower Pax5 expression. In addition, the shift between *Pax5*$^{\Delta TAD/\Delta TAD}$ and *Pax5*$^{\Delta/\Delta}$ Pax5 protein levels was not as significant as it was monitored *ex vivo* (Figure 24C).

In order to investigate the transactivation potential of the truncated Pax5 protein, Flt3 expression was examined by flow cytometric. It has been previously shown that *Flt3* is a repressed Pax5 target gene which is downregulated at the pro-B cell stage (Delogu et al. 2006). Flow cytometric analysis of the *in vitro* cultured B cells revealed that *Pax5*$^{\Delta TAD/\Delta TAD}$ B cells can repress Flt3 expression only to a certain extent (Figure 24D). However, *Pax5*$^{\Delta TAD/+}$and *Pax5*$^{+/-}$ B cells were fully capable of repressing *Flt3* (Figure 24D).

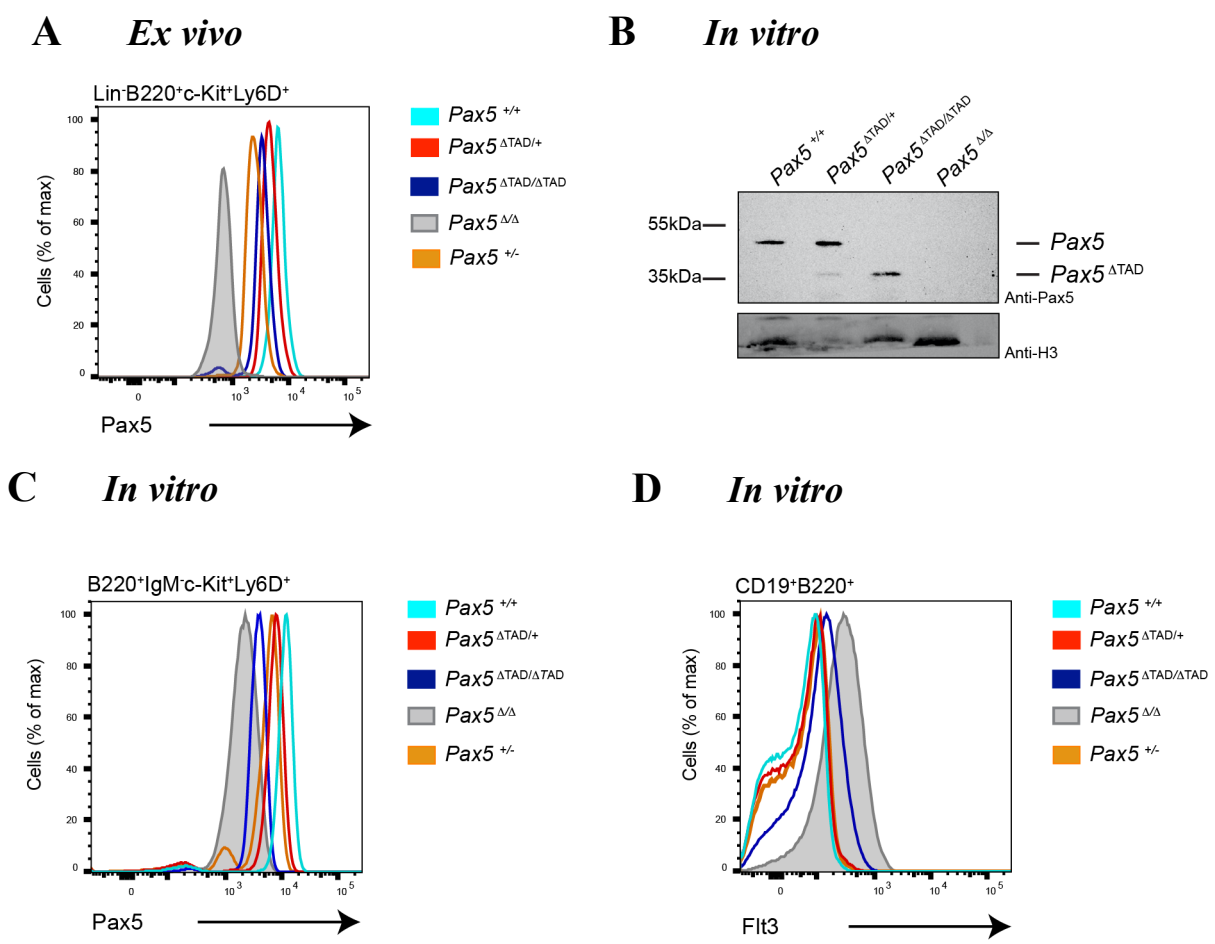

Figure 24. Expression of Pax5 in the *Pax5*$^{\Delta TAD/\Delta TAD}$ mutant.
(A) Histogram of intracellular Pax5 levels measured by flow cytometric analysis of the indicated genotypes. Pax5 levels of Lin$^-$ B220$^+$ c-Kit$^+$ Ly6D$^+$ B cells of the BM are displayed in the histogram. Similar results have been generated in 2 independent experiments. (B-D) CD19-enriched (*Pax5*$^{+/+}$, *Pax5*$^{\Delta TAD/+}$) and B220-enriched (*Pax5*$^{\Delta TAD/\Delta TAD}$, *Pax5*$^{+/-}$ and *Pax5*$^{\Delta/\Delta}$) B cells isolated from the BM of 3-week-old littermates were *in vitro* cultured on OP9 stromal cells for 10 days. Nuclear extraction and subsequent western blot analysis (B) was performed. Intracellular Pax5 levels (C) and surface Flt3 levels (D) were measured by flow cytometric analysis. (C) Similar results were generated in two independent experiments.

2.4. Generation of the *Pax5*^{REH} allele

In an ALL patient cell line termed REH, a mutation in the TAD of Pax5 has previously been identified. An additional cysteine is inserted after the first 17 amino acids in the beginning of the transactivation domain. This led to a frameshift and stop codon 19 amino acids after the C insertion, resulting in a truncated Pax5 protein (Dörfler et al. 1996). The *Pax5*^{REH} allele was generated to mimick this naturally occurring frameshift mutation (Figure 25A). The restriction site PvuII was generated upon PAM mutation (see 2.1.). After PCR amplification and *PvuII* digestion, a 596-bp WT fragment and a 294-bp and a 302-bp mutant fragment could be detected

by gel electrophoresis for genotyping (Figure 25B). The presence of the additional cysteine and the premature stop codon was verified via Sanger sequencing (Figure 2C)

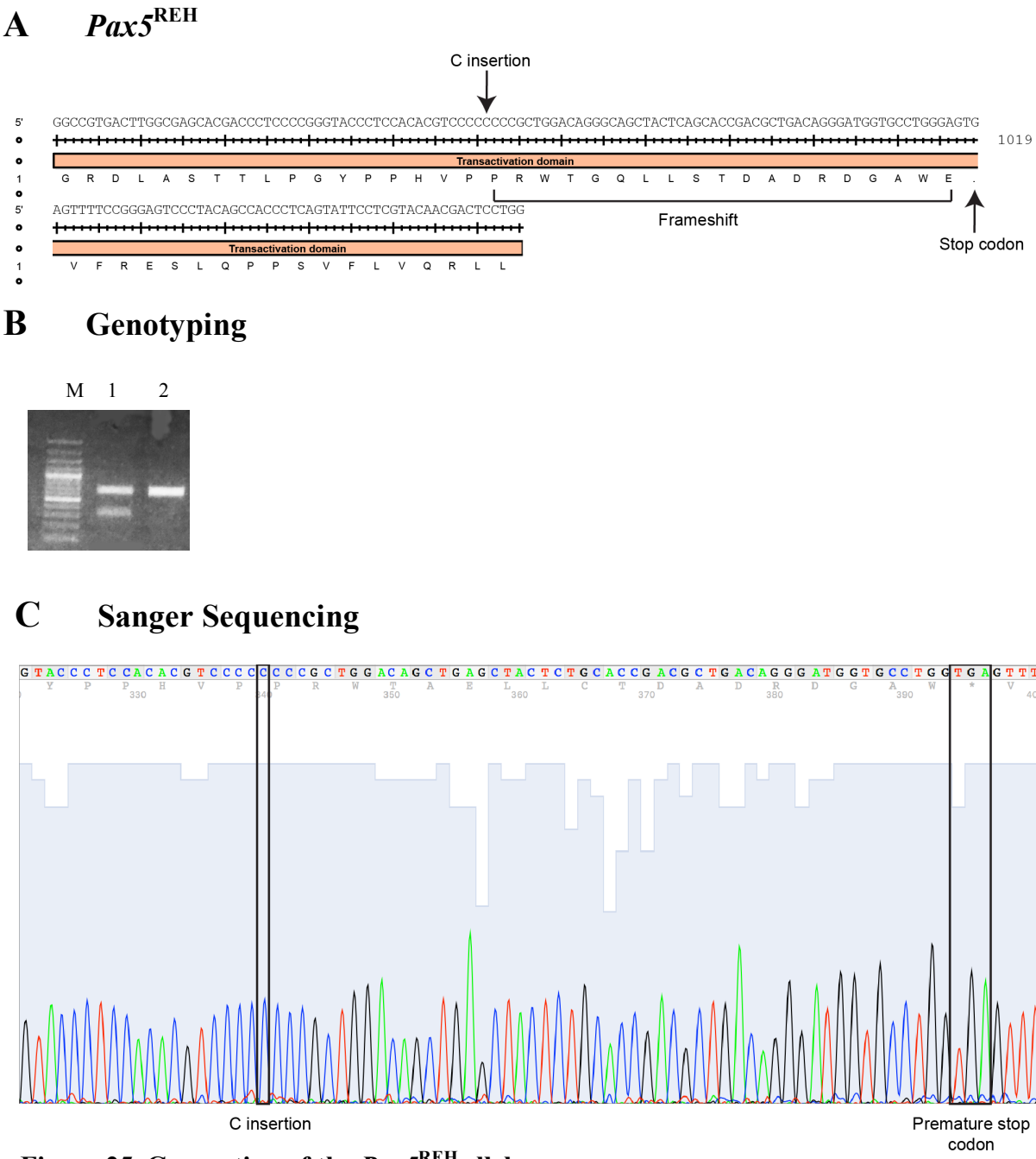

Figure 25. Generation of the *Pax5*^{REH} allele.
(A) Sequence of the *Pax5*^{REH}allele showing the cysteine insertion leading to the generation of a premature stop codon. (B) Gel electrophoresis of genotyping of *Pax5*^{REH} allele. 100-bp marker (M) was used. After PCR amplification and PvuII digest, WT and mutant band are shown. In lane 2 the WT fragment of a *Pax5*$^{+/+}$ mouse is visualized at 596-bp. The mutant fragments at 294-bp and 302-bp of a *Pax5*$^{REH/+}$ mouse are shown. (C) Sanger sequencing results verified the presence of the cysteine insertion and the premature stop codon.

2.4.1. Presence of a CD19^{+} B220^{lo} population in *Pax5*$^{REH/REH}$ mice

As it could already be observed for *Pax5*$^{\Delta TAD/\Delta TAD}$ mice, *Pax5*$^{REH/REH}$ mice showed a growth retardation. Interestingly, the growth retardation was not as severe as in *Pax5*$^{\Delta TAD/\Delta TAD}$ mice. In addition, homozygous *Pax5*$^{REH/REH}$ pups showed normal survival (data not shown). B cells of the bone marrow of 5-week-old littermates were analyzed by flow cytometry in order to examine the effect of the C-terminal truncation of the *Pax5*^{REH} mutant protein on B lymphopoiesis. Surprisingly, a CD19^{+} B220^{lo} B cell population could be identified in *Pax5*$^{REH/REH}$ mice. These cells showed a B cell developmental block at the pro-B cell stage. (Figure 26A, B). Total cell numbers revealed that *Pax5*$^{REH/REH}$ mice showed an accumulation of pro-B cells relative to WT mice. All subsequent B cell populations were absent in *Pax5*$^{REH/REH}$ mice (Figure 26A, B).

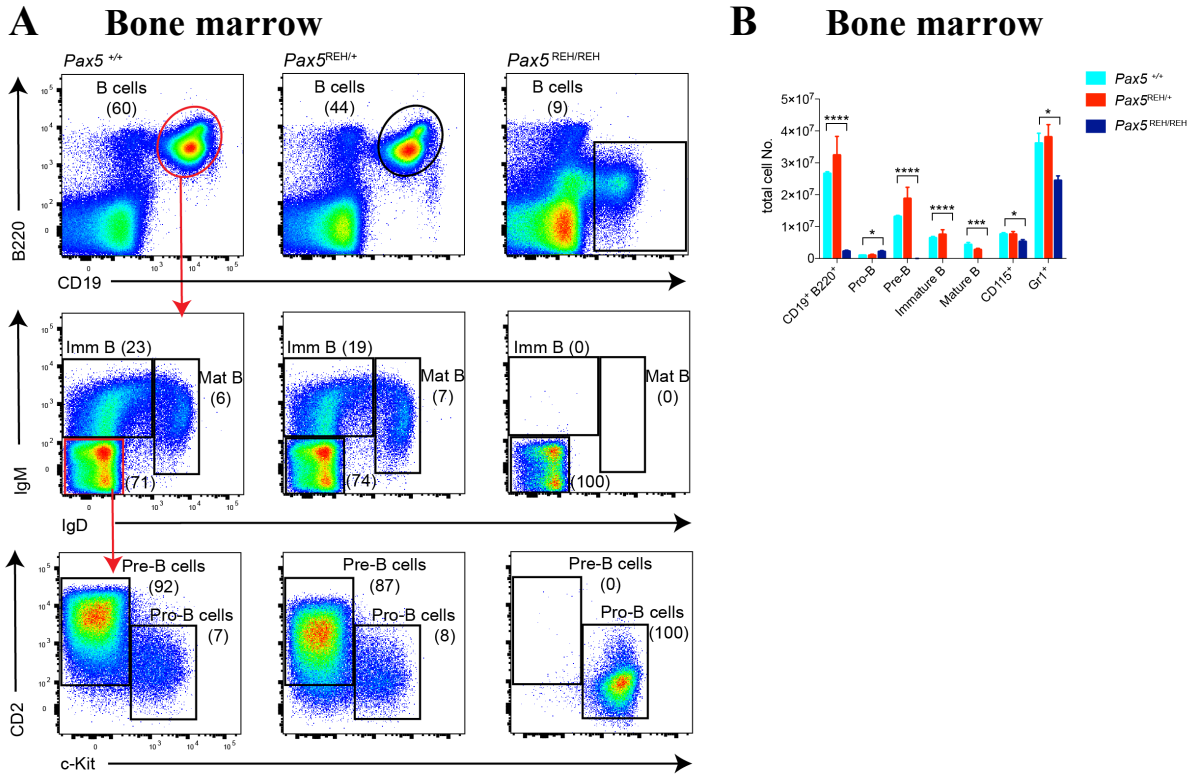

Figure 26. Presence of a CD19^{+} B220^{lo} B cell population in the BM of *Pax5*$^{REH/REH}$ mice. (A) Flow cytometric analysis of B cells isolated from the bone marrow of 5-week-old littermates of the indicated genotypes. Representative FACS plots are shown. (B) Statistical analysis of total cell numbers with mean ± S.E.M. and Welch's t-test. *, $P < 0.05$; **, $P < 0.01$; ***, $P < 0.001$; ****, $P < 0.0001$. *Pax5*$^{+/+}$ n=6, *Pax5*$^{REH/+}$n=5, *Pax5*$^{REH/REH}$ n=4.

2.4.2. B cells are absent in the spleen of *Pax5*$^{REH/REH}$ mice

B cell lymphopoiesis was also examined in the spleen of *Pax5*$^{REH/REH}$ mice and *Pax5*$^{REH/+}$ mice. They were compared to *Pax5*$^{+/+}$ splenic B cell populations. The analysis indicates that *Pax5*$^{REH/REH}$ mice did not have B cells in the spleen (Figure 27A, B). This was also reflected by a reduced spleen size in *Pax5*$^{REH/REH}$ mice (Figure 27C). In addition, reduced cell numbers of B cell subsets in the spleen could be identified in *Pax5*$^{REH/+}$ mice. (Figure 27B). T cell populations were present in the spleen and thymus of *Pax5*$^{REH/REH}$ mice (Figure 27B, D, E).

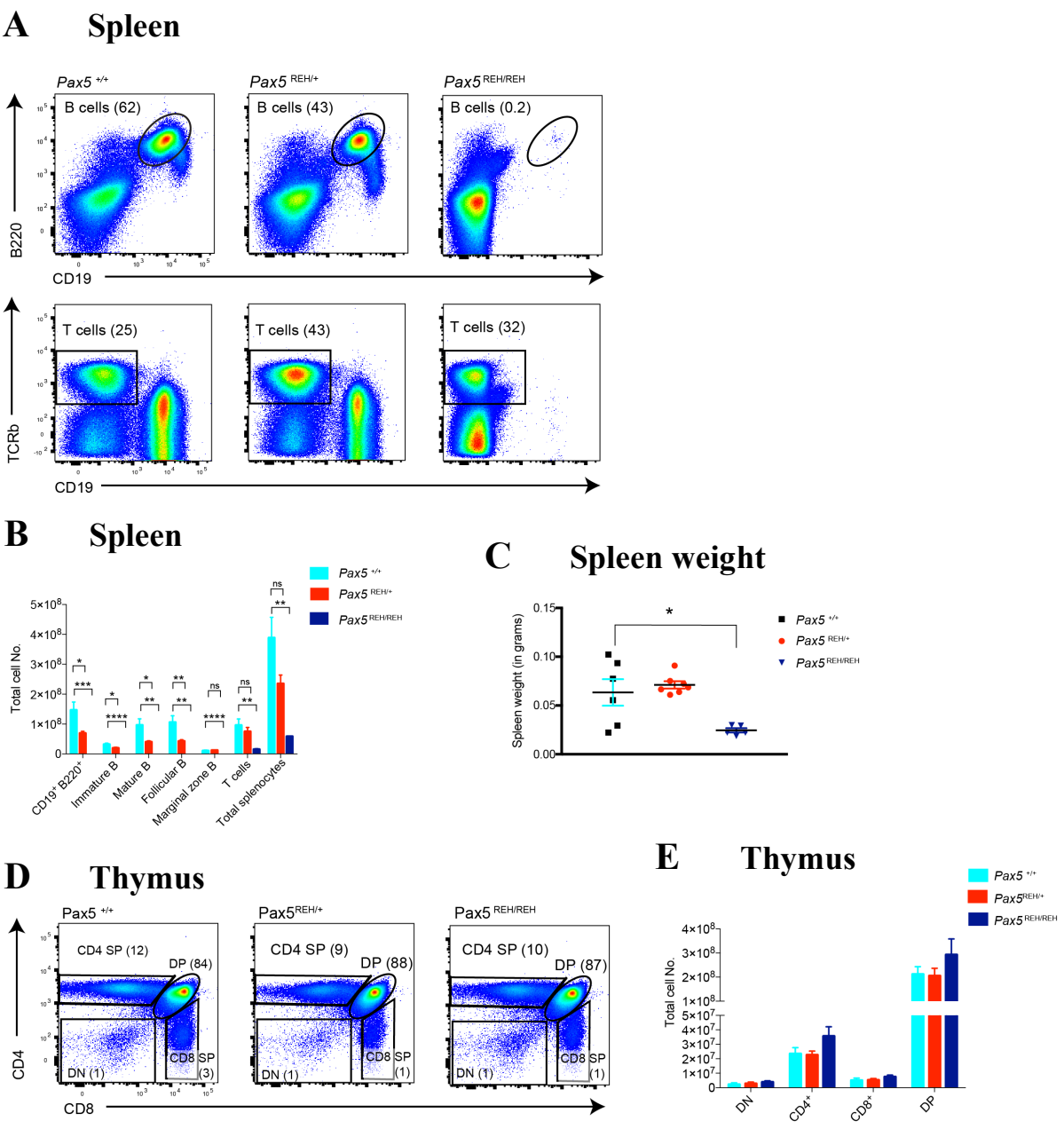

Figure 27. Absence of B cells in the spleen of *Pax5*$^{REH/REH}$ mice.
(A) Flow cytometric analysis of splenocytes of 5-week-old littermates of the indicated genotype. Representative FACS plots are shown. (B) Total cell numbers obtained with mean ± S.E.M. and Welch's t-test. *, P < 0.05; **, P < 0.01; ***, P < 0.001; ****, P < 0.0001. *Pax5*$^{+/+}$ n=6, *Pax5*$^{REH/+}$n=7, *Pax5*$^{REH/REH}$ n=5. (C) Spleen weight of *Pax5*$^{+/+}$, *Pax5*$^{REH/+}$ and *Pax5*$^{REH/REH}$ mice. Each symbol represents an individual animal. Statistical analysis has been performed with mean ± S.E.M. and Welch's t-test. *, P < 0.05. (D) Thymocytes isolated from 5-week-old littermates were examined via flow cytometry. Representative FACS plots are shown. (E) Statistical analysis on total cell numbers obtained from (D) was performed with mean ± S.E.M. *Pax5*$^{+/+}$ n=6, *Pax5*$^{REH/+}$n=6, *Pax5*$^{REH/REH}$ n=5.

2.4.3. Pax5 expression in *Pax5*$^{REH/REH}$ B cells

As stated for the *Pax5*$^{\Delta TAD}$ mutant (see 2.3.3.), intracellular Pax5 levels were analyzed via flow cytometry. To do so, pro-B cells from the bone marrow of 5-week-old littermates of *Pax5*$^{+/+}$, *Pax5*$^{REH/+}$and *Pax5*$^{REH/REH}$ mice were investigated. *Pax5*$^{REH/+}$ and *Pax5*$^{REH/REH}$ mice showed a minor decrease in Pax5 expression compared to WT Pax5 expression (Figure 28A). However, *Pax5*$^{REH/+}$ and *Pax5*$^{REH/REH}$ B cells showed a shift in Pax5 expression levels compared to *Pax5*$^{\Delta/\Delta}$ B cells (Figure 28A).

CD19-enriched bone marrow B cells (for *Pax5*$^{+/+}$, *Pax5*$^{REH/+}$) and B220-enriched bone marrow B cells (for *Pax5*$^{REH/REH}$, *Pax5*$^{+/-}$, *Pax5*$^{\Delta/\Delta}$) were *in vitro* expanded as it is described in 2.3.3. The truncated Pax5 protein of *Pax5*$^{REH/REH}$ could be identified on the western blot at 37 kDa. The ratio of the WT band and the truncated Pax5 band in *Pax5*$^{REH/+}$ mice is approximately 2:1 (Figure 28B).

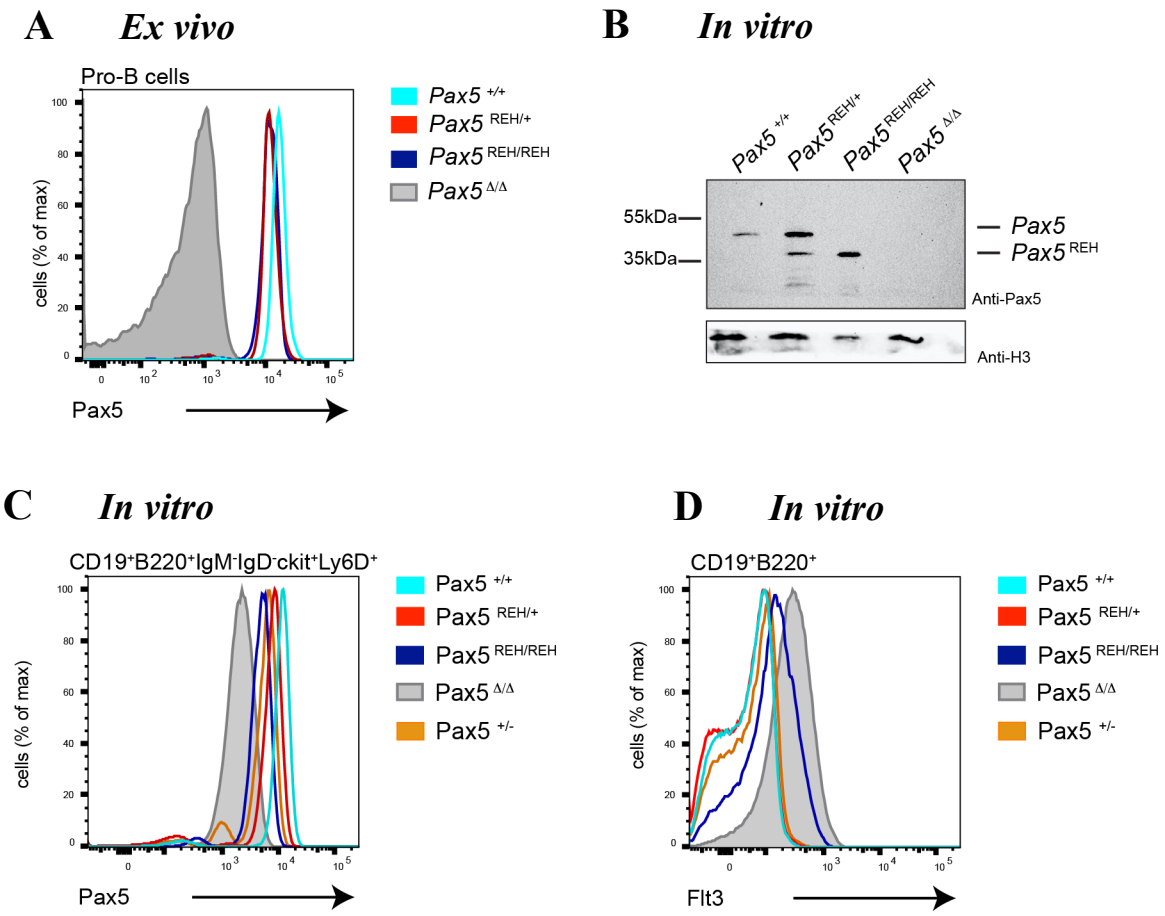

Figure 28. Expression of Pax5 in *Pax5*$^{REH/REH}$ pro B cells.
(A) Intracellular Pax5 levels of pro-B cells isolated from the BM of 5-week-old littermates of the indicated genotypes. (B-D) CD19-enriched (*Pax5*$^{+/+}$, *Pax5*$^{REH/+}$) and B220-enriched (*Pax5*$^{REH/REH}$, *Pax5*$^{+/-}$ and *Pax5*$^{\Delta/\Delta}$) B cells isolated from the BM of 4-week-old littermates were *in vitro* cultured on OP9 stromal cells for 10 days. Nuclear extraction and subsequent western blot analysis (B) was performed. Intracellular Pax5 levels (C) and surface Flt3 levels (D) were measured by flow cytometric analysis. (C) Similar results were generated in two independent experiments.

The flow cytometric analysis of intracellular Pax5 staining of the *in vitro* expanded B cells showed different results compared to the *ex vivo* data as it was also observed for *Pax5*$^{\Delta TAD/\Delta TAD}$ B cells. *Pax5*$^{REH/REH}$ B cells displayed lower Pax5 levels than *Pax5*$^{REH/+}$ B cells and *Pax5*$^{+/-}$ B cells. *Pax5*$^{REH/REH}$ B cells exhibited approximately half of the Pax5 expression as WT B cells. The expression level of Pax5 in *in vitro* cultured *Pax5*$^{REH/+}$ cells is comparable with the Pax5 level of *Pax5*$^{+/-}$ cells (Figure 28C).

In addition, Flt3 expression was monitored to investigate the repression potential of *Pax5*^{REH} protein. Low protein levels of Flt3 expression could be monitored in *Pax5*$^{REH/REH}$

which indicates that the truncated Pax5 protein was not capable of efficiently repressing *Flt3*. However, if the WT Pax5 is present on one allele, Flt3 repression was maintained (Figure 28D).

3. Discussion

Pax5 is the key player in the regulation of B cell lineage commitment and maintenance of B lymphocyte identity (Urbánek et al. 1994; Nutt et al. 1997; Cobaleda et al. 2007; Horcher et al. 2001). Various studies, on how the different Pax5 protein domains contribute to its multiple functions, have only been performed in cell lines *in vitro* so far. However, how the domains orchestrate Pax5 function *in vivo* still remains elusive. Thus, four *Pax5* mutant mouse lines have been generated in which different domains have been mutated. This study demonstrates that the MAPK phosphorylation sites and the partial homeodomain are involved in cellular processes in later B cell development upon activation of B lymphocytes. In addition, we have provided evidence that full or partial deletion of the TAD interferes with B cell development and the transactivation potential of Pax5.

3.1. The *Pax5*^{S283A,T285A} mutation might be involved in class switching

Pax5^{S283A,T258A} B cells did not show a phenotype in steady state in the BM, spleen or thymus (Figure 5). In addition, intracellular Pax5 expression levels were normal (Figure 5F). Hence, we conclude that of the MAPK phosphorylation sites serine 283 and threonine 285 are not involved in B cell development. Furthermore, it was not surprising that thymocytes populations were not affected since Pax5 is not expressed in T cells.

Upon binding of the antigen to the BCR, the kinases Lyn and Syk are activated. This induces the triggering of multiple signaling pathways such as the NF-κB pathway and the MAPK pathway (Dal Porto et al. 2004). Since previous studies revealed that S283 and T285 are phosphorylated in a MAPK-dependent manner (M. Busslinger, unpublished data) we investigated the potential effects of mutating these phosphorylation sites on B cell activation.

The expression of Pax5 and Blimp1 is mutually exclusive. Pax5 represses Blimp1 in early B cells development but upon B cell activation, Blimp1 repression is canceled and Blimp1 represses Pax5 and functions as a master regulator of plasma cell development (Lin et al. 2002; Kallies et al. 2007). Yasuda et al., hypothesized that the phosphorylation of Pax5 might be an initial event that leads to derepression of Blimp1 and subsequent repression of Pax5 by Blimp1 to induce plasma cell differentiation. ERK1/2-dependent phosphorylation of Pax5 at serines 189 and 283 was identified *in vitro* (Yasuda et al. 2012). However, this is only partially in line with previous findings of the Busslinger group, since only serine 283 and threonine 285 were

identified as MAPK-dependent phosphorylation sites (M. Busslinger, unpublished data). Yasuda et al. also claimed, that upon mutagenesis of S189 and S283, Blimp1 mRNA is reduced and therefore concluded that these two phosphorylation sites induce Blimp1 derepression (Yasuda et al. 2012). However, the intracellular Pax5 and Blimp1 staining of *in vitro* stimulated *Pax5*^{S283A,T285A} B cells did not display a defect in Pax5-Blimp1 expression kinetics (Figure 8). In addition, plasma cell populations in *Pax5*^{S283A,T285A} mice were normal upon NP-KLH immunization (Figure 9, 10). Therefore, we cannot come to the conclusion that phosphorylation of S283 and S285 is involved in regulating Blimp1 expression. This might indicate that either S189 is the initial phosphorylation site of Pax5, which induces derepression of Blimp1 or that *in vivo*, the described phosphorylation sites of Pax5 do not contribute to plasma cell differentiation as much as it was shown *in vitro*.

However, the impaired phosphorylation of Pax5 seems to be involved in class switching and cell proliferation which was not seen in previous studies. We were able to show that LPS stimulation of *Pax5*^{S283A,T285A} B cells led to significantly reduced switching to IgG3 and delayed proliferation *in vitro* (Figure 7). In line with this finding, a trend towards reduced concentration of IgM and IgG2b could be detected in the serum of NP-KLH in immunized *Pax5*^{S283A,T285A} mice (Figure 11). This will be investigated more closely via Enzyme Linked Immuno Spot assay (ELISPOT) and T-cell independent immunization (e.g. NP- Ficoll) in the future.

3.2. *Pax5*$^{\Delta HD/\Delta HD}$ mice display increased plasmablast population ex vivo and in vitro

The deletion of the partial homeodomain of the Pax5 protein did not have an effect on B cell development (Figure 13). The only alteration we could identify was that mature *Pax5*$^{\Delta HD/\Delta HD}$ B cells in the bone marrow and spleen displayed lower expression levels of IgD (Figure 13). This observation could be explained by varying cell sizes between WT and *Pax5*$^{\Delta HD/\Delta HD}$ mature B cells. Analysis of the forward scatter of the flow cytometric analysis revealed that *Pax5*$^{\Delta HD/\Delta HD}$ splenic mature B cells are slightly smaller in size when compared to WT mature B cells (data not shown). However, if cells of the same size are analyzed, IgD levels in *Pax5*$^{\Delta HD/\Delta HD}$ mature B cells were still lower in the bone marrow and in the spleen when compared to WT B cells (data not shown). The function of IgD is debated and has not been studied as intensively as IgM. Alternative splicing gives rise to expression of IgD (Geisberger

et al. 2006). It has been shown that IgM and IgD originate from the same RNA precursor from VDJ_H-rearranged *IgH* gene which can undergo alternative splicing and thus result in two distinct mRNAs coding for IgM or IgD (Moore et al. 1981). Horcher et al. identified the downregulation of IgD in mature B cells of *Pax5*$^{fl/-}$ *CD23-Cre* mice (Horcher et al. 2001). However, the expression of surface IgM was not affected. They hypothesized that this finding might indicate that Pax5 is involved in regulation of the alternative splicing of IgD mRNA (Horcher et al. 2001). This hypothesis leads to the speculation that the HD might be involved in the alternative splicing of IgD mRNA and therefore results in lower IgD levels in *Pax5*$^{\Delta HD/\Delta HD}$ mature B cells.

In addition, *Pax5*$^{\Delta HD/\Delta HD}$ B cells showed reduced class switching to IgG3 *in vitro* (Figure 15) and lower IgM and IgG2b concentrations *in vivo* (Figure 19). This might indicate that the homeodomain of the Pax5 protein could play a role in CSR directly, in signaling essential for CSR initiation or in CSR signaling for specific isotypes. Hence, closer examination on whether class switching is reduced in general or whether switching to distinct immunoglobulin isotypes is impaired, will be performed by ELISPOT analysis in the future. As mentioned in 2.2.2. mature *Pax5*$^{\Delta HD/\Delta HD}$ B cells have been analyzed using other stimulations besides LPS. However, only one mouse per genotype has been examined. Thus, other stimulations, which induce switching to other Ig isotypes, should be repeated with a greater number of replicate experiments to determine a possible effect caused by the deletion of the HD.

Interestingly, *Pax5*$^{\Delta HD/\Delta HD}$ mice displayed an elevated plasmablasts population *in vitro* and *ex vivo* upon challenging B lymphocytes (Figure 14, 18). In line with this, the Pax5 mutant mice showed a reduced population of GC B cells (Figure 17). Based on these findings, we hypothesized that the mature homeodomain deficient B cells might not reside in the GC and undergo several rounds of cell proliferation, but exit the GC earlier which would explain the accumulation of plasmablasts. Thus, we first hypothesized that the kinetics of Pax5 and Blimp1 expression might be altered. If Blimp1 is expressed prematurely, GC B cells could be rushed to terminally differentiate into plasma cells. However, intracellular staining of Pax5 and Blimp1 did not verify this hypothesis (Figure 16). Hence, investigation of other main players of plasma cell differentiation such as interferon regulatory factor 4 (IRF4), which have been previously been identified to be essential for plasma cell generation, would be of great interest (Nutt et al. 2015). In addition, it would also be interesting to analyze plasma cell and GC B cell populations *ex vivo* in unchallenged mice to investigate whether the phenotype, that we observed upon NP-KLH immunization, is already present in steady state. Moreover,

immunizing *Pax5*$^{\Delta HD/\Delta HD}$ mice with a T cell-independent reagent (NP-Ficoll) is planned for the future. This will give a closer insight whether the observed phenotype is dependent on T cell help.

Previous studies showed that TBP and RB are able to bind to the partial homeodomain of Pax5 *in vitro* (Eberhard et al. 1999). This indicates that the homeodomain of the Pax5 protein might be involved in the initiation of transcription of Pax5 target genes and cell proliferation. Hence, we want to examine TBP and RB binding of the homeodomain deficient Pax5 protein since RB is involved in cell cycle progression (Giacinti & Giordano 2006), and the possible impairment of RB binding to Pax5 might explain the delayed cell proliferation observed in *in vitro* LPS-stimulated cells (Figure 15).

3.3. *Pax5*$^{\Delta/\Delta}$ -like phenotype in *Pax5*$^{\Delta TAD/\Delta TAD}$ mice and *Pax5*$^{REH/REH}$ mice

The full or partial deletion of the TAD of *Pax5* resulted in a *Pax5*$^{\Delta/\Delta}$ -like phenotype. *Pax5*$^{\Delta TAD/\Delta TAD}$ and *Pax5*$^{REH/REH}$ mice both showed growth retardation and a B cell developmental block. However, some findings did not resemble what has previously been shown for *Pax5*$^{\Delta/\Delta}$ mice.

3.3.1. *Pax5*$^{\Delta TAD/\Delta TAD}$ mice are similar to *Pax5*$^{\Delta/\Delta}$ mice

The truncation of Pax5 in the beginning of the TAD led to a severe growth retardation, reduced spleen size and death of the pups at weaning age, as it has been shown for *Pax5*$^{\Delta/\Delta}$ mice (Urbánek et al. 1994). If the *Pax5*$^{\Delta TAD/\Delta TAD}$ pups were nurtured with wet diet, they were able to pass the critical point and survived into adulthood (data not shown).

It has been shown for *Pax5*$^{\Delta/\Delta}$ mice that Pax5 is involved in midbrain development (Urbánek et al. 1994). If *Pax5*$^{\Delta/\Delta}$ pups were lifted by their tail, they exhibit clasping of their hind limb. However, this could not be detected in *Pax5*$^{\Delta TAD/\Delta TAD}$ pups (data not shown). We therefore conclude that the deletion of the TAD of Pax5 does not interfere with neurological development.

Homozygous *Pax5*$^{\Delta TAD/\Delta TAD}$ B cells were positive for the markers B220, Ly6D, c-Kit, IL7Rα and Flt3 which suggests that they are blocked in a pre-pro-B cell stage in the bone marrow (Inlay et al. 2009). *Pax5*$^{\Delta/\Delta}$ B cells showed to be blocked in an early B cell stage (Nutt

et al. 1997) and displayed the same expression of surface marker (Figure 22). This suggests that the TAD plays an important role in B cell development *in vivo* by activating and repressing Pax5 target genes essential for B lymphopoiesis. In line with *Pax5*$^{\Delta/\Delta}$ B cell development, all subsets of B lymphocytes were absent in the spleen of *Pax5*$^{\Delta TAD/\Delta TAD}$ mice since no B cells could be detected in the bone marrow. T cells in the spleen and thymus were unaltered in homozygous *Pax5*$^{\Delta TAD/\Delta TAD}$ mice (Figure 23). This indicates that the deletion of the TAD of Pax5 does not interfere with T cell development, which was expected as Pax5 is not expressed in T cells.

In contrast to *Pax5*$^{\Delta/\Delta}$ B cells, *Pax5*$^{\Delta TAD/\Delta TAD}$ B cells expressed the truncated version of Pax5 *ex vivo* and *in vitro* (Figure 24). However, the expression level of Pax5 in homozygous *Pax5*$^{\Delta TAD/\Delta TAD}$ B cells was lower compared to WT B cells. Since B cell development in *Pax5*$^{+/-}$ mice is not affected, it was crucial to show that *Pax5*$^{\Delta TAD/\Delta TAD}$ B cells displayed higher levels of Pax5 than *Pax5*$^{+/-}$ B cells (Urbánek et al. 1994; Figure 24). This indicates that the deletion of the TAD in the Pax5 protein causes the observed B cell developmental defect and blocked B cell development is not only a result of the reduced dosage of the Pax5 protein. The different expression profiles of Pax5 in *Pax5*$^{\Delta TAD/\Delta TAD}$ B cells *ex vitro* and *in vivo* could be due to varying activity of nonsense-mediated mRNA decay, which is a control mechanism in eukaryotes that eliminates mRNAs containing a premature stop codon (Brogna & Wen 2009). Hence, we hypothesize that nonsense-mediated mRNA decay might be more active or that the truncated Pax5 protein is less stable under artificial *in vitro* culture conditions. Since the mutated Pax5 protein is expressed from the endogenous Pax5 locus, the lower expression of the truncated Pax5 protein is most likely a result of post-transcriptional modification and not due to reduced transcription of Pax5. This hypothesis could be verified by global run-on sequencing (Gro-seq) of nascent transcripts of the *Pax5*$^{\Delta TAD}$ allele since the transcripts should not be affected by nonsense-mediated mRNA decay.

Pax5$^{\Delta TAD/\Delta TAD}$ B cells were able to repress Flt3, however to a lower degree than WT and *Pax5*$^{\Delta TAD/+}$ mice. This leaves room for speculation whether other structural domains of Pax5 are also involved in its repression potential since Flt3 levels are reduced in the absence of the TAD of the Pax5 protein. Hence, investigation of additional repressed Pax5 target genes would give a closer insight whether the partial repression of Flt3 is an exception or whether this can also be observed for other repressed target genes. Furthermore, analysis of activated Pax5 target genes in *Pax5*$^{\Delta TAD/\Delta TAD}$ B cells will be performed in the future.

Intracellular Pax5 staining revealed that Pax5 levels were reduced in *Pax5*$^{\Delta TAD/+}$ B cells *ex vivo* and *in vitro* (Figure 24). The western blot also showed that the band of the truncated Pax5

protein is fainter than the WT band in the *Pax5*$^{\Delta TAD/+}$ mutant (Figure 24B). Thus, the stability of the truncated protein could be reduced in the *in vitro* expanded *Pax5*$^{\Delta TAD/+}$ B cells. However, normal B cell development could be detected by flow cytometric analysis (Figure 21). This indicates that the WT allele of Pax5 compensates for the truncated Pax5 protein on the other allele as it has been observed in *Pax5*$^{+/-}$ B cells (Urbánek et al. 1994).

3.3.2. Milder phenotype *Pax5*$^{REH/REH}$ mice in comparison to *Pax5*$^{\Delta/\Delta}$ mice

Homozygous *Pax5*$^{REH/REH}$ mice showed a milder growth retardation in comparison to *Pax5*$^{\Delta/\Delta}$ mice. However, the spleen size was significantly reduced. Interestingly, *Pax5*$^{REH/REH}$ pups showed normal survival (data not shown). In addition, *Pax5*$^{REH/REH}$ mice did not show clasping of their hind limbs when lifted by their tail (data not shown), as it was observed in *Pax5*$^{\Delta/\Delta}$ mice (Urbánek et al. 1994).

In contrast to *Pax5*$^{\Delta/\Delta}$ B cells, *Pax5*$^{REH/REH}$ B cells express CD19 in the bone marrow. This was an unexpected result since the REH mutant protein analyzed *in vitro* by Dörfler et al., showed 4-fold reduced Pax5- dependent transactivation (Dörfler et al. 1996). Furthermore, a C-terminal deletion mutant expressing the first 16 amino acids of the TAD also did not show transactivation (Dörfler et al. 1996). Hence, this provides evidence that the first 17 amino acids can induce activation of Pax5 target genes such as *Cd19, in vivo*.

However, the *Pax5*$^{REH/REH}$ B cells were blocked at the pro-B cell stage (Figure 26A, B). Splenic B cells were absent in *Pax5*$^{REH/REH}$ mice as it has been shown in *Pax5*$^{\Delta/\Delta}$ mice (Figure 27A, B). This suggests that the remaining part of the TAD is sufficient to induce CD19 expression, although B cell development was still impaired. The T cell population in the spleen and thymus were normal in *Pax5*$^{REH/REH}$ mice which indicated that the truncation of Pax5 does not interfere with T cell development (Figure 27B, D, E). As described in 3.3.1, Pax5 is not expressed in T cells and thus, no impact on T cell development was expected.

Compared to *Pax5*$^{\Delta/\Delta}$ B cells, intracellular Pax5 levels of *Pax5*$^{REH/REH}$ B cells were higher but decreased when compared to WT Pax5 levels (Figure 28A). This provides evidence that the observed phenotype is caused by the truncation of the Pax5 protein, but not by the absence of Pax5 protein. Pax5 protein levels of *Pax5*$^{REH/REH}$ B cells alter when the *ex vivo* analysis is compared to the *in vitro* experiments. As stated for full deletion of the Pax5 TAD, mRNA or protein stability might explain the fluctuating Pax5 expression levels *ex vivo* and *in vitro* in *Pax5*$^{REH/REH}$ B cells (see 3.3.1.).

In addition, it could be shown that *Pax5*$^{REH/REH}$ B cells were able to repress *Flt3,* however not to a level as it was observed in WT, *Pax5*$^{REH/+}$ and *Pax5*$^{+/-}$ B cells (Figure 28D). As it was stated for *Pax5*$^{\Delta TAD/\Delta TAD}$ mice in 3.3.1., transactivation might also be regulated by other structural domains of Pax5. The analysis of repressed and activated Pax5 target genes will be performed in the future. Thus, it will be possible to characterize the Pax5-mediated activation and repression in *Pax5*$^{REH/REH}$ B cells more closely.

3.3.3. *Pax5*$^{\Delta TAD}$ mice in comparison with *Pax5*^{REH} mice

The two Pax5 truncation mutants that have been generated are molecularly very similar since they differ only by the presence of 15 amino acids. The C-terminal truncation in the *Pax5*$^{\Delta TAD}$ mutant occurs after 2 amino acids and 4 amino acids of the frameshift at the beginning of the TAD (Figure 20A), whereas in the *Pax5*^{REH} mutant, the truncation occurs after 17 amino acids and 19 amino acids of the frameshift (Figure 25A). Despite these similarities, not the same phenotypes could be monitored.

In general, *Pax5*$^{\Delta TAD/\Delta TAD}$ mice showed a more severe phenotype that is similar to *Pax5*$^{\Delta/\Delta}$ mice, whereas the REH mutation in Pax5 displayed a milder effect. This was reflected by the survival and the growth retardation of the mice. *Pax5*$^{\Delta TAD/\Delta TAD}$ mice were severely underdeveloped and showed poor survival, while *Pax5*$^{REH/REH}$ mice displayed a minor growth defect and normal viability (data not shown). Interestingly, *Pax5*$^{REH/REH}$ pro-B cells were able to express CD19 on their surface in the bone marrow (Figure 26A) which was not observed for *Pax5*$^{\Delta TAD/\Delta TAD}$ B cells (Figure 21A). These results suggest that the 15 amino acids difference might be involved in promoting the survival of the mice and most importantly in CD19 expression which has not been shown so far. Furthermore, it can be speculated that these 15 amino acids are sufficient to induce activation of Pax5 target genes which also contribute to the survival of the *Pax5*$^{REH/REH}$ mice. However, the REH mutants also showed a block in B cell development which indicates that the 17 amino acids, which are still encoded in frame, are not capable of inducing normal B cell development (Figure 26A).

Furthermore, flow cytometric analysis of *Pax5*$^{\Delta TAD/+}$ B cells suggests that the WT Pax5 protein on one allele is able to compensate for the truncation on the other allele, as it is the case for *Pax5*$^{+/-}$ mice (Figure 21, 23). Interestingly, *Pax5*$^{REH/+}$ B cells are effected by the truncated protein on the second allele (Figure 27A, B). An explanation for this finding could be that since the *Pax5*^{REH} mutant still contains part of the TAD, the truncated *Pax5*^{REH} protein might be more competitive in terms of DNA binding than the *Pax5*$^{\Delta TAD}$ mutant and might be more successful in preventing the WT Pax5 protein to bind to DNA.

In order to study the role of the TAD in late B cell development, the two TAD truncation Pax5 mutant mice will be crossed to *Pax5*$^{fl/+}$ *CD23-Cre* mice. These mice will have normal B cell development. However, in mature B cells, the floxed Pax5 protein will be deleted. This will generate a tool to study Pax5 target genes which are activated/repressed in later stages of B cells development and might interact specifically with the TAD. In addition, comparing the two different TAD mutants in late B lymphopoiesis, can give a closer insight in which Pax5 target genes depend on the TAD domain *in vivo*.

Previous studies showed that Pax5-deficient B cells are not committed to the B cell lineage and can differentiate into other lineages of the hematopoietic system *in vitro* and *in vivo* (Nutt et al. 1999; Rolink et al. 1999; Schaniel et al. 2002). To test this *in vitro*, a co-culture system can be used. For example, *Pax5*$^{\Delta TAD/\Delta TAD}$ or *Pax5*$^{REH/REH}$ B cells can be cultured on OP-DL1 stromal cells. These cell express the Notch ligand delta-like 1 and induce T cell differentiation in uncommitted HSC (Holmes & Zuniga-Pflucker 2009). Preliminary data suggests that *Pax5*$^{\Delta TAD/\Delta TAD}$ and *Pax5*$^{REH/REH}$ B cells are not committed to the B cell lineage since they could differentiate to Thy1.2^{+} T cells upon co-culture with OP-DL1 cells (data not shown). This indicates that the full or partial deletion of the TAD in Pax5 is not sufficient to maintain B cell commitment and identity. However, additional experiments with *Pax5*$^{\Delta TAD/\Delta TAD}$ and *Pax5*$^{REH/REH}$ B cells in the presence of other lineage-specifying cytokines to induce potential dedifferentiation will be performed in the future.

The Busslinger group has performed intensive studies on the role of Pax5 in B cell development in the last years. Hence, mutant mouse strains with deletion of the paired domain or the octapeptid are available. It would be of great interest to study and compare differentially expressed genes in B cells of the paired domain mutant, the octapeptid mutant, the homeodomain mutant and the two TAD mutants of Pax5 by RNA sequencing. Thus, we would have the tool to assign activation or repression of genes specifically to the different domains of Pax5. In addition, mass spectrometry could be performed on B cells of the 5 *Pax5* mutants. By comparing the generated data of the different Pax5 mutants, it would be possible to identify Pax5 domain-specific interaction partners. This will provide closer insight into how Pax5 controls its gene expression profile *in vivo*.

3.4. Closing remarks

Taken together, considerable progress in studying the role of Pax5 in B cells has been performed so far. Nevertheless, how the various structural domains of Pax5 contribute to its

multiple functions in B cell lymphopoiesis *in vivo* still remains elusive. With this study, we could provide a closer insight into the complexity of the role of Pax5 in B cell development. We were able to provide evidence that the partial homeodomain and the phosphorylation of Pax5 at S283 and T285 are involved in activation *in vivo*. In addition, we were able to show that the TAD of Pax5 is essential for B cell development and commitment *in vivo*. However, there are still open questions, which need to be addressed in the future in order to further characterize the molecular mechanism of Pax5 function and its interaction partners.

4. Experimental procedures

4.1. Mouse strains

All four *Pax5* mutant mouse lines have been generated by Louisa Hill and Daniela Kostanova-Poliakova of the Busslinger group. The mouse strains were generated by CRISPR/Cas9-mediated genome editing in mice zygotes performed by the "Transgenic service" core facility provided by the Research Institute of Molecular Pathology/ Institute of Molecular Biotechnology.

4.1.1. Genotyping

Tail buffer
0.1% SDS
200 mM NaCl
100 mM Tris pH 8.0
5 mM EDTA

10x Taq buffer
100 mM Tris pH 8.3
500 mM KCl
15 mM $MgCl_2$

Toe clipping of the mice was performed for genotyping. Toes were incubated with Tail buffer and 20mg/ml proteinase K (VWR) overnight at 55˚C. DNA was precipitated with isopropanol. Sample was centrifuged at 13.000 rpm for 10' at room temperature. The pellet was dried and resuspended in TE.

Genotyping PCR

Per reaction:		PCR program:	
19.7µl	H_20	94˚C, 3'	
2.5µl	10x Taq buffer	94˚C, 0.30'	⎫
0.5µl	dNTPs (NEB)	58˚C, 0.30'	⎬ Repeat 37x
0.5µl	primer A	72˚C, 0.50'	⎭
0.5µl	primer B	72˚C, 5'	
0.3µl	Taq polymerase (in- house)	12˚C, ∞	
0.5µl	DNA		

Restriction digest of PCR product

25µl	PCR reaction
42µl	H_20
5µl	10x restriction buffer (NEB)
2µl	restriction enzyme (NEB)

Restriction digest was incubated at least 3 hours at 37˚C.

Primers used for genotyping

Genotype	Primer A	Primer B
Pax5^{S283A,T285A}	CTCTTGTGATGCTGTGTGGG	GACAGAAGGACTAGGTGGTGC
Pax5$^{\Delta HD}$	CTCCTTTGGTGGTGGGATAGC	CTGTGTCCAGCAAACTGACC
Pax5$^{\Delta TAD}$	CTCGAGGGGGTGCTGATTTC	GAGGTCACCTGGACTGCTTT
Pax5^{REH}	CAAGTAGAGCCAGGGTAGCTG	AAGTCCCTTGTCAGCCACAC

4.1.2. Sanger Sequencing

For cloning, TOPO TA cloning Kit for Sequencing (Invitrogen) was used. Cloning was performed as stated in the manufacturer's manual. Plasmid DNA was isolated via Miniprep Kit (Qiagen) as stated in the manufacturer's manual. Samples were sequenced by the in house Sanger sequencing service provided by the molecular biology service of the Research Institute of Molecular Pathology/ Institute of Molecular Biotechnology.

4.2. Definition of cell types

Bone marrow

B cells	$CD19^+$ $B220^+$
Pro-B cells	$CD19^+$ $B220^+$ IgM^- IgD^- $CD2^-$ $c\text{-}Kit^+$
Pre-B cells	$CD19^+$ $B220^+$ IgM^- IgD^- $CD2^+$ $c\text{-}Kit^-$
Immature B cells	$CD19^+$ $B220^+$ IgM^+ IgD^-
Mature B cells	$CD19^+$ $B220^+$ IgM^- IgD^+

Progenitor cells in bone marrow	
Pre-pro-B cells	$Lin^- B220^+ Flt3^+IL7Ra^+Ly6D^+ c\text{-}Kit^+$ (Lin: CD3, CD4, CD8, CD11b, DX5, Gr1, Ly6C, Ter119 and NK1.1)
Spleen	
B cells	$CD19^+ B220^+$
Immature B cells	$CD19^+ B220^+ IgM^+ IgD^{lo}$
Mature B cells	$CD19^+ B220^+ IgM^{lo} IgD^{hi}$
MZ B cells	$CD19^+ B220^+ IgM^{hi} IgD^{lo} CD21^{hi} CD23^{lo/-}$
FO B cells	$CD19^+ B220^+ IgM^{lo} IgD^{hi} CD21^{int} CD23^{hi}$
GC B cells	$CD19^+ B220^+ Fas^+ GL7^+$
Plasma cells	$Lin^- B220^{in} CD138^{hi} CD28^+$ (Lin: CD4, CD8, CD11b, CD21, DX5)
Lymph nodes	
GC B cells	$CD19^+ B220^+ Fas^+ GL7^+$
Plasma cells	$Lin^- B220^{in} CD138^{hi} CD28^+$ (Lin: CD4, CD8, CD11b, CD21, DX5)
Thymus	
DN	$CD4^- CD8^-$
DP	$CD4^+ CD8^+$
CD8 SP	$CD4^- CD8^+$
CD4 SP	$CD4^+ CD8^-$

4.3. Isolation of Cells

2.5-to 8-week-old mice were sacrificed using a CO_2 chamber. Subsequently, pelvis, tibia, femora, spleen, thymus and lymph nodes were extracted. Spleen, thymus and lymph nodes were stored in ice cold PBS containing 2% FCS and 2.0 mM EDTA (FACS buffer) and kept on ice. Via pistil and mortar, the bone marrow was isolated by crushing the bones. The spleen, thymus and lymph nodes were mashed using the back of a 10ml syringe. In order to maintain single cell suspension, the obtained cell suspensions were filtered through a 70µm cell strainer.

4.4. FACS Analysis

Ex vivo isolated cells or *in vitro* harvested cells were stained with listed, commercially available FACS antibody. The FACS antibodies were diluted in FACS buffer (PBS, 2% FCS, 2mM EDTA) containing Fc block (1:500).

Bone marrow

Antibody	clone	Supplier
CD19	1D3	BD Bioscience
B220	RA3-6B2	BD Bioscience
IgM	II/41	eBioscience
CD2	RM2-5	Biolegend
c-Kit	2B8	eBioscience
IgD	11.26c	eBioscience
CD115	AFS98	eBioscience
TCRb	H57-597	BD Bioscience
Gr1	RB6-8C5	eBioscience
Ter119	Ter119	Biolegend

Progenitors

Antibody	clone	Supplier
Flt3	A2F10	eBioscience
Strepdavidin		Biolegend
IL7Ra	A7R34	eBioscience
Ly6D	49-H4	Pharmingen
B220	RA3-6B2	Biolegend
ScaI	Ly6A/E	BD Bioscience
c-Kit	2B8	Biolegend
CD3	17A2	Biolegend
CD4	GK1.5	eBioscience
CD8	53-6.7	eBioscience
CD11b	M1/70	Pharmingen
CD49b	DX5	Biolegend
Gr1	RB6-8C5	eBioscience
Ly6C	HK1.4	Biolegend
Ter119	TER-119	eBioscience
NK1.1	PK136	Biolegend

Intracellular Pax5 staining

Antibody	clone	Supplier
CD19	1D3	BD Bioscience
B220	RA3-6B2	BD Bioscience
IgM	II/41	eBioscience
CD2	RM2-5	Biolegend
c-Kit	2B8	eBioscience
IgD	11.26c	eBioscience
Pax5	1H9/ D19F8	Thermo Scientific/ Cell Signaling
Flt3	A2F10	eBioscience
ScaI	Ly6A/E	BD Bioscience
Ly6D	49-H4	Pharmingen
c-Kit	2B8	Biolegend
CD3	17A2	Biolegend
CD4	GK1.5	eBioscience
CD8	53-6.7	eBioscience
CD11b	M1/70	Pharmingen
CD49b	DX5	Biolegend
Gr1	RB6-8C5	Biolegend
Ly6C	HK1.4	Biolegend
Ter119	TER-119	eBioscience
NK1.1	PK136	Biolegend

Intracellular Pax5-Blimp1 staining

Antibody	clone	Supplier
CD138	281-2	BD Bioscience
CD22	B3B4	Pharmingen
Strepdavidin		Biolegend
CD19	1D3	BD Bioscience
IgG3	R40-82	Pharmingen
Pax5	D19F8	Cell Signaling
Blimp1	5E7	BD Bioscience

In vitro LPS-stimulated B cell

Antibody	clone	Supplier
CD138	281-2	BD Bioscience
CD22	B3B4	Pharmingen
CD19	1D3	BD Bioscience
IgG3	R40-82	Pharmingen

Spleen

Antibody	clone	Supplier
CD21	7 E9	Biolegend
B220	RA3-6B2	Biolegend
CD19	1D3	eBioscience
IgM	II/41	eBioscience
CD23	B3B4	Biolegend
IgD	11.26c	eBioscience
TCRb	H57.597	Biolegend

Thymus

Antibody	clone	Supplier
CD8	53-6.7	Biolegend
CD44	IM7	Biolegend
B220	RA3-6B2	BD Bioscience
Thy1.2	30-H12	eBioscience
CD25	PC61	Pharmingen
c-Kit	2B8	eBioscience
CD4	GK1.5	eBioscience

Plasmablast

Antibody	clone	Supplier
CD28	37.51	eBioscience
CD138	281-2	Pharmingen
B220	RA3-6B2	Biolegend
CD4	GK1.5	eBioscience
CD8	53-6.7	eBioscience
CD11b	M1/70	eBioscience
CD21	7G6	Biolegend
CD49b	DX5	eBioscience

Germinal Center B cells

Antibody	clone	Supplier
Fas	Jo2	BD Bioscience
GL7	GL7	eBioscience
CD19	1D3	eBioscience
B220	RA3-6B2	Biolegend
IgG1	A85-1	BD Bioscience

4.4.1. Intracellular staining

Intracellular staining of Pax5 and Blimp1 was performed using the Foxp3/ Transcription Factor Staining Buffer Set (ThermoFisher). After surface staining of the cells, fixation reagent (1:3 in fixation diluent) was added to the cells and incubated for 1 hour at 4˚C. Cells were washed twice with permeabilization buffer. Subsequently, cells were stained with Pax5 (1H9, Thermo Scientific) directly coupled to PE. For the intracellular staining of the *Pax5*$^{\Delta HD}$ mutants or the *in vitro* LPS-stimulated cells, Pax5 (D19F8, Cell Signaling) and Blimp 1 (5E7, BD Bioscience) coupled to PE were used. Since rabbit-Pax5 (D19F8, Cell Signaling) is not coupled to a fluorophore, anti-rabbit IgG coupled to APC (Cell Signaling) was added.

4.5. Tissue culture

4.5.1. Pro- B cell culture

OP9 medium

IMDM

10% FCS
1% L-Glu
1% Pen/Strep
50 mM b-mercaptoethanol

B cell medium

IMDM
2% FCS
1% L-Glu
1% Pen/Strep
50 mM b-mercaptoethanol
10% Primatone
IL7
SCF

OP9 stromal cell were splitted by trypsinization every second day (approximately $0.8x10^6$ cells/ 15cm cell culture plate) and were plated on 6 cm ($1.4x10^5$ cells) or 10 cm ($4x10^5$ cells) sterile cell culture plates. If OP9 cells are not plated the day before, at least 2-3 hours were waited in

order to let them settle. On the next day, mice were sacrificed as described in (see 4.3). Femur, tibia and hip of both legs of the mice were crushed in ice cold FACS buffer using autoclaved pistil and mortar. A single cell suspension was generated by pipetting up and down. The cells were filtered through a 70mm cell strainer into a 50ml falcon tube. Subsequently, the cells were enriched for CD19 or B220 via magnetic activated cell sorting (MACS) (Miltenyi Biotec). OP9 medium was exchanged to B cell medium prior to plating the pro-B cells. The medium was exchanged every day and cells were passaged to bigger cell culture plates, if they were confluent enough. If the 15cm cell culture plate was confluent, pro-B cells were harvested, pelleted and frozen at -80˚C until they were used for nuclear extraction (see 4.6). In addition, part of the harvested cells was used for FACS analysis.

4.5.2. *In vitro* LPS stimulation of B cells

Stimulation medium

IMDM
10% FCS
1% L-Glu
1% Pen/Strep
50 mM b-mercaptoethanol
LPS (25µl/ml)

6- 8-week-old mice were sacrificed and lymph nodes and spleen were harvested. The organs were mashed in FACS buffer and the single cell suspension was filtered through a 70µm cell strainer. Subsequently, the cells were depleted for CD43 via MACS (Miltenyi Biotec). Cell ($0.5x10^6$ cells/ml) were either plated in a 6-well cell culture plate or stained with CellTrace Violet™ (Invitrogen). Hence, 1µl CellTrace Violet™ was used with 1ml PBS to stain $1.5x10^6$ cells. Cells were incubated for 20’ at 37˚C and washed twice with PBS prior to plating on a 6-well cell culture plate. FACS analysis was performed 4 days after plating.

4.6. Nuclear Extraction

Succrose-buffer
0.32 M sucrose
10 mM Tris pH 8.0
50 mM KCl
20 mM NaCl
3 mM $CaCl_2$
2 mM $MgCl_2$
1 mM Dithiotreitol (DTT)
2 mM 6- aminocaprois acid (6AA) : chymotrypsin inhibitor
0.15 mM sperimine
0.5 mM spermidine
protease inhibitor cocktail (PIC)
with or without 0.2% NP-40

Low salt buffer
10 mM Hepes pH 7.9
20% glycerol
20 mM KCl
2 mM $MgCl_2$
2 mM 6AA
0.5 mM DTT
PIC

Highsalt buffer
10 mM Hepes pH 7.9
20% glycerol
700 mM KCl
2 mM $MgCl_2$
2 mM 6AA
0.5 mM DTT
1% NP-40

Cells were thawed on ice and pelleted (300 RCF, 5' at 4˚C). Pellet was resuspended in 50µl sucrose buffer per 10^7 cells. Equal volume of sucrose buffer + 0.2% NP40 was added. Nuclei were pelleted (500 RCF, 10' at 4˚C) and subsequently washed with 1ml sucrose buffer (without NP-40). Nuclei were pelleted (500 RCF, 10' at 4˚C) and resuspended in low salt buffer (20µl for $1x10^7$ cells, 50µl for $5x10^7$ cells, 200µl for $1x10^8$ cells). 1/5 volume of high salt buffer was added slowly while constantly shaking (gently) of the sample. 1/5 volume of high salt buffer was continuously added until 1 volume was added. Benzonase exonuclease was added (450U per $2x10^8$ cells). Sample was incubated for 45' at 4˚C. The nuclear lysate was centrifuged at 16,000 RCF for 10' at 4˚C. The supernatant was carefully transferred to a fresh tube and centrifuge at 16,000 RCF for 45' at 4˚C. The supernatant was again transferred to a fresh tube. The nuclear extracts were stored at -80˚C.

4.7. SDS-PAGE and Western blot

2x Lämmli sample buffer

5% (w/v) SDS
25% (v/v) glycerol
150 mM Tris-HCl pH 6.8
0.01% (w/v) bromophenol blue
0.7 M β-mercaptoethanol

Nuclear Extracts were incubated with 2x Lämmli sample buffer for 5' at 95˚C. Nuclear extracts were subsequently fractioned by SDS-PAGE. For blotting, proteins were transferred from the gel to a PDVF membrane. Blocking of the membrane was performed for 1 hour at room temperature in PBS-T (0.1% Tween) and 3% milk powder while constantly shaking. Primary antibody was added in PBS-T and 3% milk powder and incubated over night at 4˚C. Subsequently, membrane was washed 3 times and membrane was incubated with secondary antibody in PBS-T and 3% milk powder for 1 hour at room temperature. Membrane was washed 3 times. Proteins were detected via chemiluminescence.

4.8. ELISA

Blocking buffer
PBS
1% BSA
0.05% Tween

ELISA buffer
PBS
0.1% BSA
0.05% Tween

Maxisorp plate was coated with 1μg/ml isotype-specific goat- anti-mouse antibodies (Southern Biotech). Plates were incubated for 2h (or overnight) at 37˚C. 200μl/ well of the blocking buffer was added and incubated 2h at 37˚C. Plates were washed with PBS 3 times. Serial dilutions in ELISA buffer (1:200) of sera of NP-KLH immunized mice were generated. As a standard, pooled sera of the immunized mice were used and diluted in the same manner. Plates were incubated 2h at 37˚C and washed with PBS 3 times. 1μg/ml of the secondary antibody (alkaline phosphatase-linked, Southern Biotech) was added. Plates were incubated 2h at 37˚C and washed with PBS 3 times. After washing, pNPP Substrate (Southern Biotech) was added. Concentrations were measured by microwell-plate reader at 405nm.

4.9. Immunization of mice with NP-KLH

100μg NP-KLH (1μg/μl) in alumn were injected intraperitoneal in the mouse. Spleen and lymph nodes were analyzed 14-days post injection.

4.10. Statistical analysis

Calculation of mean ± S.E.M. was performed by Welchs's t-test using licensed Prism 7 (GraphPad). *, $P < 0.05$; **, $P < 0.01$; ***, $P < 0.001$; ****, $P < 0.0001$.

5. Zusammenfassung

B Lymphozyten sind Teil des Hämatopoetischen Systems. Diese Zellen sind in der Lage hoch-affine Antikörper zu produzieren, welche die humorale Immunität gegen fremde Pathogene bilden. Das Eintreten der B Zelle in die B Zelllinie, findet in dem pro-B-Zell-Stadium statt. Die B-Zell-Entwicklung wird durch zahlreiche externe Signale und Transkriptionsfaktoren kontrolliert, wie zum Beispiel das paired box protein 5 (Pax5). Der multifunktionale Transkriptionsfaktor Pax5 führt eine duale Rolle in der B-Zell-Entwicklung aus: es unterdrückt die Expression von nicht-B Zell-spezifischen Genen und aktiviert gleichzeitig B Zell-spezifische Gene. Dadurch induziert Pax5, dass B Zellen in der B Zelllinie bleiben und kontrolliert die Aufrechterhaltung der B-Zell-Identität während der B-Zell-Entwicklung.

Das Protein Pax5 besteht aus mehreren konservierten Domänen, welche bis jetzt nur in Zelllinien *in vitro* genauer charakterisiert wurden. Um die Funktion der Domänen *in vivo* zu untersuchen, wurden vier verschiede Mauslinien generiert, in denen Pax5 in unterschiedlicher Weise mutiert wurde. Zwei Pax5 Mauslinien wurden hergestellt, indem entweder die Homeodomäne deletiert wurde, oder zwei mitogen-activated protein kinase- (MAPK) Phosphorylierungsstellen mutiert wurden. Obwohl die B-Zell-Entwicklung in diesen Mäusen normal verläuft, kommt es durch Lipopolysaccherid (LPS) Stimmulation *in vitro* und durch 4-Hydroxy-3-Nitrophenyl Acetyl- Schlitzschnecken Hämocyanin (NP-KLH) Immunisierung *in vivo* zu einer fehlerhaften B-Zell-Aktivierung. Der Phosphorylierungs- Mutante zeigte eine reduzierte Zellteilung *in vitro* und niedrigere Level an Immunoglobulin (Ig)M, IgG3, IgG2b. Interessanterweise, konnte in der Pax5 Mutante mit der deletierten Homeodomäne, weniger Plasmablasten *in vitro* detektiert werden. Dies konnte auch *in vivo* in Verbindung mit weniger Keimzentrum B Zellen beobachtet werden.

Zusätzlich, wurden zwei weitere Pax5 Mutanten generiert, die Beide ein verkürztes Pax5 Protein exprimieren. Eine Mutante zeigt eine Verkürzung des Pax5 Proteins am Anfang der C-terminalen Transaktivierungsdomäne, die andere Mutante expremiert jedoch noch einen Teil der Transaktivierunsdomäne. Die Deletion der ganzen Transaktivierungsdomäne zeigte einen Arrest in der frühen B Zellentwicklung, welches bereits in Pax5-defizienten B Zellen beobachtet werden konnte. Unerwarteterweise, zeigte die andere Pax5 Mutante CD19 Expression. Jedoch, ist auch in dieser Mutante die B-Zell-Entwicklung in einem frühen Stadium blockiert.

6. Abstract

B lymphocytes are part of the hematopoietic system and are crucial for generating high-affinity antibodies, which provide humoral immunity against foreign pathogens. B cell lineage commitment is initiated at the pro-B cell stage and is maintained throughout B lymphopoiesis. B cell development is controlled by a multitude of external signals and transcription factors, including the paired box protein 5 (Pax5). The multifunctional transcription factor Pax5 fulfills a dual role in B cell development: it represses non-B cell lineage genes and simultaneously activates B cell lineage-specific genes. By doing so, Pax5 induces B cell commitment and controls the maintenance of B cell identity throughout B cell development. Importantly, B-lymphopoiesis is arrested at an early uncommitted progenitor stage in the absence of Pax5.

The Pax5 protein is composed of several conserved domains, which have so far only been characterized in cell lines *in vitro*. To investigate the function of these domains by mutagenesis *in vivo*, we generated four different *Pax5* mutant mice lacking individual domains. Two *Pax5* mutant mouse lines have been generated in which either the homeodomain was deleted in frame or two mitogen-activated protein kinase (MAPK) phosphorylation sites were mutated. Although B cell development was normal in these mice, *in vitro* stimulation of mature B cells with lipopolysaccharide or *in vivo* stimulation with 4-hydroxy-3-nitrophenyl acetyl-keyhole limpet hemocyanin (NP-KLH) revealed impaired B cell activation. The phosphorylation mutant displayed delayed cell proliferation *in vitro* and decreased levels of the immunoglobulin isotypes IgG3, IgM and IgG2b *in vitro* and *in vivo*, respectively. Interestingly, the Pax5 mutant in which the homeodomain was deleted showed a decreased percentage of activated B cells and increased plasmablasts upon LPS stimulation. In line with this, less germinal center (GC) B cells and higher levels of plasmablasts could be detected in the spleen and lymph nodes post NP-KLH immunization. In addition, decreased switching to IgG3, IgM and IgG2b could be observed *in vitro* and *in vivo*.

In addition, two mutant mouse strains, containing a frameshift mutation leading to a truncated Pax5 protein lacking the C-terminal transactivation domain to different degrees, were generated. Complete deletion of the C-terminal transactivation domain resulted in a developmental arrest at the onset of B-lymphopoiesis, which was similar to that of the *Pax5* knockout mice. The presence of the first few amino acids of the transactivation domain in the second mouse mutant facilitated the activation of selected Pax5 target genes such as *Cd19*, but still showed an arrest in B cell development at a pro-B cell-like stage.

7. References

Adams, B. et al., 1992. Pax-5 encodes the transcription factor BSAP and is expressed in B lymphocytes, the developing CNS, and adult testis. *Genes Dev*, 6, pp. 1589 – 1607

Adolfsson, J. et al., 2005. Identification of Flt3+ Lympho-Myeloid Stem Cells Lacking Erythro-Megakaryocytic Potential. *Cell*, 121(2), pp.295–306.

Brogna, S. & Wen, J., 2009. Nonsense-mediated mRNA decay (NMD) mechanisms. *Nature Structural & Molecular Biology*, 16(2), pp.107–113.

Busslinger, M. & Tarakhovsky, A., 2014. Epigenetic control of immunity. *Cold Spring Harbor Perspectives in Biology*, 6(6), pp.a019307–a019307.

Cobaleda, C.S. et al., 2007. Pax5: the guardian of B cell identity and function. *Nature Immunology*, 8(5), pp.463–470.

Dal Porto, J., 2004. B cell antigen receptor signaling 101. *Molecular Immunology*, 41(6-7), pp.599–613.

De Silva, N.S. & Klein, U., 2015. Dynamics of B cells in germinal centres. *Nature Rev. Immunology*, 15(3), pp.137–148.

Delogu, A. et al., 2006. Gene Repression by Pax5 in B Cells Is Essential for Blood Cell Homeostasis and Is Reversed in Plasma Cells. *Immunity*, 24(3), pp.269–281.

Dörfler, P. et al., 1996. C-terminal activating and inhibitory domains determine the transactivation potential of BSAP (Pax-5), Pax-2 and Pax-8. *EMBO J.*, 15, pp.1971–1982

Eberhard, D. et al., 1999. The partial homeodomain of the transcription factor Pax-5 (BSAP) is an interaction motif for the retinoblastoma and TATA-binding proteins. *Cancer Res.*, 59, pp.1716–1724

Eberhard, D. et al., 2000. Transcriptional repression by Pax5 (BSAP) through interaction with corepressors of the Groucho family. *EMBO J.*, 19, pp.2292–2303.

Fuxa, M. et. al., 2004. Pax5 induces V-to-DJ rearrangements and locus contraction of the immunoglobulin heavy-chain gene. *Genes and Development*, 18, pp.411-422.

Fuxa, M. et al., 2007. Reporter gene insertions reveal a strictly B lymphoid-specific expression pattern of Pax5 in support of its B cell identity function. *The Journal of Immunology*, 178(5), pp.3031–3037.

Geisberger, R., Lamers, M. & Achatz, G., 2006. The riddle of the dual expression of IgM and IgD. *Immunology*, 118, pp.429-437

Giacinti, C. & Giordano, A., 2006. RB and cell cycle progression. *Oncogene*, 25(38), pp.5220–5227.

Holmes, R. & Zuniga-Pflucker, J.C., 2009. The OP9-DL1 System: Generation of T-Lymphocytes from Embryonic or Hematopoietic Stem Cells In Vitro. *Cold Spring*

Harbor Protocols, 2009(2), pp.pdb.prot5156–pdb.prot5156.

Horcher, M., Souabni, A. & Busslinger, M., 2001. Pax5/BSAP Maintains the Identity of B Cells in Late B Lymphopoiesis. *Immunity*, 14(6), pp.779–790.

Inlay, M.A. et al., 2009. Ly6d marks the earliest stage of B-cell specification and identifies the branchpoint between B-cell and T-cell development. *Genes & Development*, 23(20), pp.2376–2381.

Kallies, A. et al., 2007. Initiation of plasma-cell differentiation is independent of the transcription factor Blimp-1. *Immunity*, 26(5), pp.555–566.

Kurosaki, T., Kometani, K. & Ise, W., 2015. Memory B cells. *Nature Rev. Immunology*, 15(3), pp.149–159.

Li, Y.-S., 1996. Identification of the Earliest B Lineage Stage In Mouse Bone Marrow. *Immunity*, (5), pp. 552-535.

Lin, H. & Grosschedl, R. Failure of B-cell differentiation in mice lacking the transcription factor EBF. *Nature* 376, pp.263–267.

Lin, K.I. et al., 2002. Blimp-1-Dependent Repression of Pax-5 Is Required for Differentiation of B Cells to Immunoglobulin M-Secreting Plasma Cells. *Molecular and Cellular Biology*, 22(13), pp.4771–4780.

Lin, Y. et al., 1997. Repression of c-myc Transcription by Blimp-1, an Inducer of Terminal B Cell Differentiation. *Science*, 267, pp.596-599.

Lin, Y.C. et al., 2010. A global network of transcription factors, involving E2A, EBF1 and Foxo1, that orchestrates B cell fate. *Nature Immunology*, 11(7), pp.635–643.

Maul, R.W. & Gearhart, P.J., 2010. AID and Somatic Hypermutation. In Advances in Immunology. Elsevier, pp. 159–191.

McManus, S. et al., 2011. The transcription factor Pax5 regulates its target genes by recruiting chromatin-modifying proteins in committed B cells. *The EMBO Journal*, 30(12), pp.2388–2404.

Medvedovic, J. et al., 2011. *Pax5: A Master Regulator of B Cell Development and Leukemogenesis* 1st ed., Elsevier Inc.

Moore, K. W. et al., 1981. Expression of IgD may use both DNA rearrangements and RNA splicing mechanism. *Immunology*, 78(3), pp.1800-1804.

Minnich, M. et al., 2016. Multifunctional role of the transcription factor Blimp-1 in coordinating plasma cell differentiation. *Nature Immunology*, 17(3), pp.331–343.

Murphy, K. et al., 2007. Janeway's Immunobiology (7th Edition). *Garland Science, Taylor & Francis Group, LLs.*

Nagasawa, T., 2006. Microenvironmental niches in the bone marrow required for B-cell development. *Nature Reviews Immunology*, 6(2), pp.107–116.

Nutt, S.L. et al., 1997. Essential functions of Pax5 (BSAP) in pro-B cell development: difference between fetal and adult B lymphopoiesis and reduced *V*-to-*DJ* recombination at the *IgH* locus. *Genes Dev.*, 11, pp.476–491.

Nutt, S.L., 1999. Commitment to the B-lymphoid lineage depends on the transcription factor Pax5. *Nature* 401, 556–562.

Nutt, S.L. & Kee, B.L., 2007. The transcriptional regulation of B cell lineage commitment. *Immunity*, 26(6), pp.715–725.

Nutt, S.L. et al., 2015. The generation of antibody-secreting plasma cells. *Nature Rev. Immunology*, 15(3), pp.160–171.

Parker, D.C., 1993. T Cell-Dependent B Cell activation. *Annu. Rev. Immunology*, 11, pp.331-360.

Piskurich, J. F. et al., 2000. BLIMP-I mediates extinction of major histocompatibility class II transacti- vator expression in plasma cells. *Nat. Immunol*. 1, pp.526–532.

Rickert, R.C. et al., 1997. B lymphocyte-speci c, Cre-mediated mutagenesis in mice. *Nucleic Acids Res.*, 25, pp.1317–1318.

Rolink, A.G. et al., 1999. Long- term in vivo reconstitution of T-cell development by Pax5-deficient B-cell progenitors. *Nature*, 401, pp. 603–606.

Schaniel, C. et al., 2002. Multiple hematopoietic cell lineages develop in vivo from transplanted Pax5-deficient pre-B I-cell clones. *Blood*, 99, pp.472–478.

Schwenk, F. et al. 1997. Generation of Cre recombinase-specific monoclonal antibodies, able to characterize the pattern of Cre expression in cre-transgenic mouse strains. *Journal of Immunological Methods*, 207, pp.203-212.

Shikh, El, M.E.M. et al., 2010. Activation of B cells by antigens on follicular dendritic cells. *Trends in Immunology*, 31(6), pp.205–211.

Urbánek, P. et al., 1994. Complete block of early B cell differentiation and altered patterning of the posterior midbrain in mice lacking Pax5/BSAP. *Cell*, 79, pp901 – 912.

Yasuda, T. et al., 2012. B Cell Receptor-ERK1/2 Signal Cancels PAX5-Dependent Repression of BLIMP1 through PAX5 Phosphorylation: A Mechanism of Antigen-Triggering Plasma Cell Differentiation. *The Journal of Immunology*, 188(12), pp.6127–6134.

Zhuang, Y. et al., 1994. The Heli-Loop-Helix Gene E2A Is Required For B Cell Formation. *Cell*, (79), pp. 875-884.